INTERRELATIONSHIPS BETWEEN SATELLITE-OBSERVED CLOUD PATTERNS, NUMERICALLY ANALYZED BAROCLINICITY, AND VERTICAL MOTION

JAMES WESLEY SHOEMYER

INTERRELATIONSHIPS BETWEEN SATELLITE-OBSERVED CLOUD PATTERNS, NUMERICALLY ANALYZED BAROCLINICITY AND VERTICAL MOTION

by

James Wesley Shoemyer
Lieutenant Commander, United States Navy
B.S., University of Missouri, 1952

Submitted in partial fulfillment of the
requirements for the degree of

MASTER OF SCIENCE IN METEOROLOGY

from the

NAVAL POSTGRADUATE SCHOOL
June 1967

ABSTRACT

Numerically analyzed baroclinicity, an operational product of Fleet Numerical Weather Facility (FNWF), Monterey, California, is related to cloud patterns depicted on ESSA III nephanalyses for the Atlantic-European and Pacific-North American areas during the period 7-17 December 1966. In addition, interrelations between the numerically analyzed fronts, satellite cloud observations and FNWF 850-mb and 500-mb vertical motion fields are presented.

Hyperbaroclinic zones are found to contain a greater percentage of clouds than areas outside these zones at all latitudes from 15-60 N. For instance, 61% (44%) of the average hyperbaroclinic zone in the Pacific-North American (Atlantic-European) area is covered by more than .5 clouds while only 30% (28%) of the adjacent quasi barotropic zones show similar cloudiness. The FNWF fronts and cloud bands are found to be most closely related, in orientation and intensity, in the dense-data Atlantic Ocean area. More clouds are found to occur in regions of ascent than in regions of descent, the ratio being 2 over land and 1.5 over ocean areas, but the correlation of vertical motion and percentage of cloud cover is not simple or necessarily positive.

TABLE OF CONTENTS

LIST OF TABLES

LIST OF ILLUSTRATIONS

Legend:

Numerically located front (from FNWF GGθ analysis)

M

Point of GGθ maximum greater than .15 C/(100km)^2 but less than .20 C/(100km)^2

Region of GGθ maximum with central value equal to or greater than .20 C/(100km)^2

Figure Page

Boundaries of major cloud patterns (cloud amount covered)

Boundaries of mostly covered cloud patterns

Vortex

PVA MAX

Legend: Same as figure 10, except,

M — Location of GGθ maximum greater than .15 C/(100km)^2

••••• — 850-mb vertical motion contours: 0 and 1 cm sec^{-1} Areas greater than 1 cm sec^{-1} are shaded

– – – — 500-mb vertical motion contours: 0 and 1 cm sec^{-1} Areas greater than 1 cm sec^{-1} are shaded

(+2.2) — 850-mb vertical velocity in cm sec^{-1}

+2.2 — 500-mb vertical velocity in cm sec^{-1}

ACKNOWLEDGEMENTS

Appreciation is expressed to Associate Professor Robert J. Renard of the Naval Postgraduate School, Monterey, California, for his guidance and assistance. Appreciation is also expressed to the staff at Project FAMOS, Fleet Weather Central, Washington, D. C., for assistance in obtaining nephanalyses and to Leo Clarke, Fleet Numerical Weather Facility, Monterey, California, for providing the GGθ analyses used in this investigation.

1. Introduction

Hemispheric objective frontal analyses have been produced by Fleet Numerical Weather Facility (FNWF) Monterey, California, for the past two and one-half years. This operational product, developed by Renard and Clarke [13] , is based on a front-location parameter given the name GGθ. The parameter, applied to temperature data on constant pressure surfaces, may be defined as the directional derivative of the magnitude of the gradient of potential temperature (θ) along the gradient of θ. In the current model the potential temperature field is obtained by computing the thickness of the layer from 1000 to 700 mb and converting it to a mean potential temperature for the layer [8] . The ridges (axes of maximum values) of GGθ in a field thus obtained become the warm-air boundaries of the 1000-mb hyperbaroclinic zones[1] and coincide closely with conventional 1000-mb fronts, while the troughs (axes of minimum values) of GGθ are rear or cold-side boundaries of the zones [13] . The ridge and trough values have been shown to correlate well with the strength of baroclinicity in the transition zones [6] . Figure 1 is a typical operational FNWF frontal analysis. As noted, only the positive values of the GGθ field are contoured, allowing the location of the warm-air boundaries of frontal zones only.

During the period that the FNWF frontal analyses have been operationally produced, several investigations were conducted in an effort to find if any definite relationship exists between the numerically analyzed baroclinicity and cloud patterns.

---

[1] Hereafter "hyperbaroclinic" zones will be simply referred to as "baroclinic" zones while the areas outside these zones will be called "quasi barotropic".

McCord [10] investigated the correlation between the FNWF frontal analyses and the National Meteorological Center (NMC) nephanalyses as derived from TIROS X and ESSA I weather satellite observations. This study comprised a five-day period in January 1966 and a two-day period in February 1966.

For the first phase of his study, McCord compared cloud masses and bands[2] to both baroclinic and quasi barotropic zones and concluded that although baroclinic zones are cloudier than quasi barotropic zones, the difference is slight. The second phase of his study was restricted to a comparison between baroclinic zones possessing $GG\theta$ values exceeding a certain minimum value of the $GG\theta$ parameter and satellite observed cloud bands. Here, McCord concluded that such cloud bands occur in both quasi barotropic and baroclinic zones, the latter being favored only slightly.

McCord conducted an additional study relating FNWF 850-mb and 500-mb vertical motion analyses to satellite observed cloud patterns. From these results he concluded that there is good correlation between the existence of cloud bands and vertical ascent.

Shoemyer and Tupaz [15] investigated the relationship between the FNWF frontal analyses and the NMC nephanalyses based on the ESSA I observed cloud patterns for a six day period in March 1966. This study led to the conclusion that there is a definite association between the FNWF fronts and those cloud bands designated as "frontal" on

---

[2]See Appendix I for definition of this and other technical weather satellite terminology.

the NMC nephanalyses, but the results were inconclusive for other cloud bands and masses. All of the studies just reviewed indicate a need for further investigation in this area with the recommendation that more extensive tests be conducted.

2. Objectives

The prime objective of this thesis study was to conduct a more extensive investigation of the relationship between the FNWF numerically analyzed baroclinicity and satellite-observed clouds. A second objective was to study further the aforementioned products in relation to the FNWF 850-mb and 500-mb vertical motion analyses.

The cloud, frontal and vertical motion analyses are products available to the operational Navy Meteorologist. Their efficient use, either singly or in conjunction with one another, would certainly be enhanced by knowledge of usable relations between these products. Thus, the final objective was to make recommendations that may aid the practicing Navy Meteorologist to make optimum use of these products.

3. Background

The Glossary of Meteorology describes a frontal zone as the region in which density and moisture gradients are relatively large while the front is a line of intersection between the warm-side boundary of the frontal zone and a constant pressure, horizontal or other surface. Such a frontal zone of concentrated baroclinicity may be considered a region between two quasi barotropic air masses. This concept is basic to the interpretation of the GGθ analyses.

Cloud patterns associated with frontal phenomena are dependent upon the slope or inclination of the frontal surface, vertical velocities, and stability conditions in and adjacent to the baroclinic zones. Much has been written on the location of clouds and cloud systems with respect to the various classes and types of frontal systems. The earlier relationships, as determined by conventional analyses, are presented in the Handbook of Meteorology [3]. Later, Bergeron, in 1951, presented a model of weather systems which are usually associated with large scale vertical motions in frontal-wave cyclones and associated anticyclones [12]. The availability of satellite observed cloud data in recent years has resulted in numerous investigations regarding the interpretation of these data and their relationship to conventional frontal analyses. In general, these investigations have found the recurrence of similar cloud, vertical motion and frontal features [1, 4]. One of these studies presents an excellent and typical depiction of the clouds associated with an active frontal system and is reproduced here as figure 2 [1].

Since the ridges in the GGθ analyses define the positions of the low level fronts, it was anticipated that the relationships between the GGθ fronts and cloud patterns would be similar to those found between conventionally analyzed fronts and cloud patterns as reported in the aforementioned studies. Testing to determine the validity of this statement was one of the objectives of this study. At the outset, however, one major difference was apparent when comparing the conventional front to the GGθ front; namely, the GGθ analysis does not consistently depict occlusions partly due to the lack of baroclinicity associated with

occlusions in lower levels [8, 10, 15]. Work is currently in progress at FNWF and the Naval Postgraduate School (PGS), Monterey, California, which will allow occlusions to manifest themselves on the GGθ analyses.

Inasmuch as cloud patterns associated with frontal activity are closely associated with vertical motion fields, a brief discussion of numerical fronts and related vertical motion is included in this report. The synoptic scale vertical motions computed by FNWF result primarily from vorticity and thermal advection processes involving the thermal wind and hence the baroclinicity. Both FNWF 850-mb and 500-mb vertical motion analyses were used in this phase of the investigation.

Most previous workers in this field have found a somewhat complex association between vertical motion, frontal phenomena and clouds. Hadfield [7] found that the vertical motion patterns associated with frontal passages varied from front to front. Krishnamurti et al [9] presented a frequent pattern of sky cover that is observed in the occlusion stage of a certain type of extratropical frontal cyclone. He also found that the upward vertical motions at 500-mb related to this pattern are not primarily determined by the same mechanisms in all regions. Further, Sanders [14] found that centers of ascent and descent tended to occur within the baroclinic zones downstream and upstream of the progressive mid-tropospheric troughs, respectively, rather than in adjacent air masses. The scale of Sanders' baroclinic zones compare quite favorably with those derived from the GGθ analysis, although the lateral boundaries of his baroclinic zones were arbitrarily considered to lie where the intensity of the horizontal temperature gradient dropped to one-half the maximum value in the zone.

Though the vertical motion relationship to frontal activity is not a simple one, most investigators generally agree that clouds are associated with, but by no means coincident with, regions of upward vertical motions.

4. Area and Time of Study and Related Matters

Initially the study was confined to a comparison of the cloud features of the NMC nephanalyses to the location and degree of baroclinicity on the FNWF GGθ analyses for the eleven-day period from 7 through 17 December 1966. This period was not chosen because of the occurrence of any unusual weather phenomena during the time of the study but solely because of the availability of the data.

The December 1966 weather was characterized by abnormally strong zonal flow at 700-mb over much of the Northern Hemisphere with mean troughs near both coasts of North America. See figures 3 and 4 [5]. This same pattern was generally true during the period 7 through 17 December. Specifically, in the Pacific area of concern, a series of cyclones with related frontal systems traversed the Pacific in the latitude band 40-55N during the time interval 7 through 11 December. From 12 through 17 December, the pattern was generally the same, except the paths of the lows were nearer 40-45N in the western Pacific, the lows subsequently curving northeast into the Gulf of Alaska. In the Atlantic, the storm tracks were confined to polar latitudes due to the presence of a relatively strong stationary subtropical high at latitudes north of normal. Because of this, only the trailing portions of fronts crossed into the Atlantic area of study. Over Europe and Asia the weather in the early part of the period was dominated by a high pressure cell over Siberia and weak lows in the Mediterranean. The weather in the latter days of the period was generated mainly by low cells in the North Sea and over the northern part of the continent with frontal activity across Europe extending southward to the Mediterranean area.

Complete hemispheric satellite nephanalysis coverage from ESSA III was available for the period studied, however, the FNWF frontal analyses are computed only at the radiosonde-observation times, 0000 and 1200 GMT. A portion of a typical nephanalysis is shown in figure 5. In order to consider a significantly large area while at the same time keeping the cloud and baroclinicity analyses essentially concurrent, only the neph-analyses within four hours of the 0000 and 1200 GMT synoptic times were utilized. During early phases of the research, nephanalyses within three hours of 0000 and 1200 GMT were used, but it was found that this led to a restricted area of coverage in the North Atlantic Ocean. Consequently, periods within four hours of the frontal analysis times were selected. Cloud data were collected such that those within three and four hours of map time could be considered separately. Upon analysis of the data it became apparent that the cases involved in the questionable one-hour interval would have no detrimental effect on the overall result. As a consequence, in the final analysis, no distinction was made between the three-hour and four-hour time intervals and the statistical results are based on nephanalyses within four hours of the FNWF frontal analyses.

Utilization of the nephanalyses within four hours of 0000 and 1200 GMT led to two geographical areas of study (figure 6). The time interval around 0000 GMT gave coverage over most of the North Pacific Ocean plus a portion of the western North American Continent. The interval around 1200 GMT gave coverage of the eastern North Atlantic Ocean, Europe, and part of Asia. Though the east and west boundaries of the zones varied slightly from day to day, due to satellite photographic coverage, they are generally as shown in figure 6. Since the seasonally-imposed northern limit of the NMC nephanalysis is about 55 to 60N and the FNWF

frontal analysis is not contoured below 15N, the latitudinal boundaries of the areas of study were chosen accordingly. These geographical areas were further subdivided for ease in handling data as well as distinction between land and ocean areas and/or sparse and dense data areas. Furthermore, the areas were divided zonally in 15 degree latitude bands between 15N and 60N for ease in handling data; this also gives an indication of the distribution of baroclinicity with latitude. The data density subdivision was based upon the average density of surface and 500-mb reports received at FNWF [8]. Figures 7 and 8 show typical coverage at the surface and 500-mb levels. Actual data density for the period of study was not available. The area subdivisions are shown as A through F in figure 6. As noted from figures 6, 7 and 8, area A is a relatively dense-data ocean area as compared to the sparse-data ocean area E. Of the remaining areas, B and F are dense data land-areas, while C and D are comparatively sparse-data areas.

Since the FNWF frontal analyses, as shown in figure 1, can be used only to locate the ridges in the GGθ field, the FNWF computer printouts of the GGθ fields were used in collecting data for this study. An example of the printout is shown in figure 9. By analyzing the troughs and ridges in the field, baroclinic and quasi barotropic areas can be located. The baroclinic zone is that area between a ridge and trough on the cold air side of the GGθ ridge. Conversely, the quasi barotropic areas are found between the ridge and trough on the warm air side of GGθ ridge.

5. Satellite Observed Clouds versus FNWF Frontal Analyses (Phase I)

a. Introduction

The study of clouds and baroclinicity was divided into two phases. The first phase was a general investigation of both cloud

masses and bands as related to baroclinic and quasi barotropic zones, while the second was concerned only with major cloud bands and their relations to baroclinic and quasi barotropic zones. Section 6 is devoted to Phase II.

In an attempt to "zero-in" on the relationship between clouds and baroclinic and/or quasi barotropic zones this phase of the investigation took two avenues of approach. First, determine what portion of each 15 degree latitude band, described earlier, is baroclinic and quasi barotropic and estimate the percentage cloud cover in each of these regions. Next, considering all cloud masses and bands, determine what portion of each lies in baroclinic and quasi barotropic zones.

The results of the first approach are summarized in Tables 1 and 2. Table 1 applies to the Pacific area and Table 2 to the Atlantic-European area. The results of the second approach are summarized in Tables 3 through 6. Tables 3 and 4 summarize the data for cloud bands and cloud masses, respectively, in the Pacific area. Tables 5 and 6 summarize the same data for the Atlantic-European area. The area subdivisions indicated by the letters A through F are in accordance with those described in figure 6.

In Tables 1 and 2, the second column, entitled AVG $GG\theta$, $C/(100km)^2$, expresses the average values of the ridges and of the troughs obtained in each of the various zones for the entire eleven-day period. The next column indicates what portion of each 15 degree latitude band is baroclinic and what portion quasi barotropic. The fourth column heading indicates the percentage of cloud coverage in the corresponding baroclinic areas and the values in the last column indicate the same for quasi barotropic areas. Note that only covered (C) and mostly covered (MCO) cloud regions were considered; clouds in mostly open (MOP) and

open (O) areas were not included in the study. The averages tabulated in the last row of Tables 1 and 2 are not merely arithmetic averages of the figures in each column, but are weighted averages based upon the relative sizes of each latitude band.

The columns headed TYPE CLOUD BAND AND COVERAGE in Tables 3 and 5 and the columns headed TYPE CLOUD MASS AND COVERAGE in Tables 4 and 6 separate the clouds into three categories. FRONTAL COVERED refers to cloud in the amount C which is designated as frontal on the nephanalysis. All other clouds in the amounts C and MCO are included in the two NON-FRONTAL categories. No cases of FRONTAL MOSTLY COVERED were encountered.

In Tables 3 and 5, the angles in the columns AVG ANGLE BETWEEN THE GGθ RIDGE AND CLOUD BAND were obtained by measuring the angle between the cloud band axis and that GGθ ridge which appeared to be closely related to the cloud band. These angles varied widely and their range is included in the succeeding column. Column 6 entitled AVG GGθ $(C/(100km)^2)$ VALUE IN RIDGE, gives the average values of GGθ found in the related ridges. The percentages in the final column are the average portions of the cloud bands that were found in baroclinic and quasi barotropic zones.

Tables 4 and 6 give the same data for clouds masses as are given in Tables 3 and 5 for cloud bands with the exception, for obvious reasons, of the angular information.

In summary, for Phase I, areas of baroclinicity and quasi barotropy have been located, the amount of clouds in these areas has been estimated and the results recorded in Tables 1 and 2. Conversely, the cloud patterns were located and related to baroclinicity and the results are contained in Tables 3 through 6. A discussion of results follows.

b. Results

Before commencing a discussion of the results of Phase I of the study, it should be pointed out that the cloud statistics presented here pertain to cloud amount only. That is, no attempt was made, on the basis of the nephanalyses, to make any distinction between high, low, and middle clouds. An exception to this procedure occurred for the cases of cloud bands or masses composed entirely of cirriform cloud. Such clouds were not considered to have any direct relation to low level baroclinic zones and thus were not considered in the statistics.

With reference to Table 1 for the Pacific areas, the average amount (column 3) and relative magnitudes of baroclinicity (column 2) are indicated for each of the latitude bands cited in column 1. The higher numbers in the "ridge" column compared to the "trough" column indicate that the warm side boundaries of baroclinic zones represent more of a thermal discontinuity than the cold side boundaries. Also, the magnitude of the average $GG\theta$ values along the ridges and troughs, a measure of the strength of the baroclinicity, increases with latitude. Tropical latitudes are associated with the least percentage of baroclinic zones, with the two higher latitude baroclinic regions having approximately the same percentage (average of 35%). These results are consistent with climatology and the weather pattern for this particular period as discussed in section 4.

Covered (C) cloud areas definitely increase poleward; the same conclusion is not so clear for mostly covered (MCO) areas. Baroclinic zones average 41% covered while quasi barotropic zones average only 19% covered. Again the MCO category has little differentiation in each zone.

It is to be noted that C and MCO combined comprise an average of 61% of baroclinic zones but only 30% of quasi barotropic zones, with the ratio at low latitudes (high latitudes) exceeding (falling short of) the ratio of 61/30. At middle and high latitudes 77% or more of the baroclinic zones are C + MCO while in low and mid latitudes 41% or less of the quasi barotropic zones are covered by C + MCO.

In the Atlantic-European areas (see Table 2) the average value of GGθ at the ridges and troughs increases with latitude in a way similar to the Pacific areas. However, there is an apparent difference in the percentage of baroclinic zones in each of the latitude bands when compared with the latter areas. In the Atlantic-European regions, the lowest latitude zone has the highest percentage (39%) of baroclinicity. This zone is just south of the mean winter position of the Mediterranean front [11] . A perusal of the FNWF frontal analyses shows the presence of a GGθ ridge at a latitude of about 15N to 20N on all days during the period 7-17 December. The average GGθ value of this ridge is relatively low and its maximum value was seldom found to be over .15C/(100km)^2. There is relatively little low and middle cloudiness that could be associated with these baroclinic zones (25%). As with the Pacific, C areas increase poleward but baroclinic zones average 31% covered (C) while quasi barotropic zones are 16% covered. The ratio of C + MCO in baroclinic zones to quasi barotropic zones is 44/28 compared to 61/30 in the Pacific. These ratios reduce to 1.6 (Atlantic) versus 2.0 (Pacific). The cloud amounts in each zone are less in the Atlantic-European than in the Pacific. In the Atlantic-European area it is only at high latitudes that C + MCO approaches 3/4 coverage (actually 74%) while all latitude bands show C + MCO less than 38% in quasi barotropic zones.

In summary, Tables 1 and 2 demonstrate that the average amount of cloudiness (C or C+MCO) in the baroclinic zones at all latitudes is considerably larger (almost by a factor of 2) than the amount of cloudiness in the quasi barotropic zones at corresponding latitudes or for the combination of all latitudes. However, in agreement with climatology, cloudiness increases with latitude, both for baroclinic and quasi barotropic zones.

An examination of Table 3 shows that in the Pacific area E, the average angle between the cloud bands and their associated GGθ ridges is larger (29° versus 15°), and has a wider range (10-90° versus 5-45°), in the cases of frontal clouds than in cases of non-frontal bands. As was mentioned earlier, the FNWF frontal analysis does not adequately depict occlusions. This fact is a possible explanation for the wide range and large average values of the angles; that is, when the occlusion is not depicted, the GGθ ridge will imply amplitudes consistent with an unoccluded wave while the associated cloud band shows amplitude and orientation consistent with an occluded front. Corresponding values in Atlantic area A of Table 5 appear to disagree with this, since the average angle in the frontal covered category is small (14°). As was noted in a preceding paragraph, the storm track in the Pacific was well within the area studied from 7 through 17 December. At the same time in the Atlantic area, the path was generally north of the area covered by the nephanalyses. Confirming these facts, a perusal of the NMC surface charts in these two areas for the period of this study shows twenty one occluded systems in the Pacific area versus only four in the Atlantic. Thus, it would seem that the information obtained for the Atlantic verifies, rather than contradicts, that obtained in the Pacific.

Further examination of Tables 3 and 5 discloses that in the frontal covered category a greater portion of the cloud band fell into the baroclinic zone than in the quasi barotropic zone in both ocean areas A and E, but the cloud amount in the quasi barotropic zone is by no means insignificant. With reference to the model in figure 2, this statistic is not unexpected as frontal bands are generally prefrontal for the rapidly moving segment of fronts while post frontal clouds are common near the quasi stationary portion. In the non-frontal C and MCO classes a greater portion of the average cloud band is found in the barotropic zone in area E; however, in area A the average cloud band was nearly equally distributed between the barotropic and baroclinic zones. Additionally, in both ocean areas, the average magnitude of the $GG\theta$ ridges associated with the cloud bands is higher for frontal covered than for non-frontal covered, which speaks well for selection of "frontal" bands by the nephanalysts. Non-frontal mostly covered is associated with the weaker baroclinic zones. Regarding the cloud bands as listed in order of decreasing significance for each area in Tables 3 and 5, it is of interest to note the correlation of average $GG\theta$ values with these bands.

There is insufficient data for frontal cloud bands over the land areas to be of any significance. However, the non-frontal covered cloud bands in the land areas B and C do appear to show slight preference for baroclinic compared to quasi barotropic zones. The non-existence of frontal covered in area C, with apparently high values of $GG\theta$, makes questionable the nephanalysts' labels in this region.

Tables 4 and 6 display the relation between cloud masses and baroclinicity for the entire period of study. In all ocean areas the greater portion of the average cloud mass fell into the quasi barotropic area. The same was true of the land area B; however, in land areas C and F,

the greater part of the average cloud mass was in the baroclinic zone. It is difficult to assess significance to these figures, especially since greater than two-thirds of the area considered is quasi barotropic and since the cloud mass category has little direct association with elongated zones of intense thermal gradients either in orientation, location, or structure. However, it is apparent that in the Pacific region the frontal band is embedded in the "mass" on many occasions which precludes the separation given by the "mass" and "band" categories.

6. Satellite Observed Clouds versus FNWF Frontal Analyses (Phase II)

a. Introduction

The second phase of the study was confined to a comparison of the major GGθ ridges and related major cloud bands. GGθ ridges evidenced by the contouring on the operational FNWF frontal analysis (see figure 1) were considered major. The five-day period, 13 through 17 December 1966, was selected for study in the Pacific area while the period,11 through 15 December 1966, was investigated in the Atlantic-European area. In view of the fact that these periods fall within the period described in Phase I, the weather pattern discussed therein remains valid for Phase II. These two five-day periods are considered to be representative of the main period, 7 through 17 December. Additionally, the geographical boundaries of the areas involved are identical to those shown in figure 6.

Tables 7 and 8 report the results of this particular investigation. Table 7 summarizes the data for the Pacific area while Table 8 does the same for the Atlantic-European area. The data for calculating the values in the tables were obtained from the computer printout versions of GGθ (see figure 9) after comparing the computer printout to the operational frontal analysis (figure 1) in order to determine the major GGθ ridges

or fronts. The AVG GGθ VALUES were found in the same manner in which similar values were found in the preceding tables. The average lengths of the GGθ ridges or fronts expressed in the next column are simply an average of all ridges studied. The final columns in Tables 7 and 8 indicate the average amount of major cloud banding as found in the baroclinic and quasi barotropic zones adjacent to the major GGθ ridges.

In summary, Tables 7 and 8 give an indication of the degree of baroclinicity and dimensions of baroclinic and quasi barotropic zones associated with major GGθ ridges as well as the average amount of clouds in major cloud bands in these zones. A discussion of results follows.

b. Results

As noted in Tables 7 and 8, an equal number of cases in each area were considered with the average GGθ ridge values nearly the same (.25 and .29). Although the frontal lengths average 49 degrees latitude the range of this parameter varied from 20 degrees to more than 110 degrees latitude; in fact, many bands spanned the full width of the areas of study. The tables also indicate that there is a greater amount of cloud banding in the baroclinic zone than in the adjacent quasi barotropic zone (75% vs 61% in Pacific; 54% vs 47% in Atlantic areas). Reasons for this have been discussed already with reference to the model in figure 2.

Though Tables 7 and 8 give some idea of the relation between the major GGθ ridges and major clouds, certainly this relation could be represented more dramatically in a graphical depiction. This has been done in figures 10A through 10E and 11A through 11E. These figures illustrate the relation between the FNWF frontal analyses and the major satellite observed clouds for the Pacific and Atlantic-European areas, respectively. Only covered and mostly covered clouds are included in the figures.

Comparison of cloud patterns to numerical fronts in regions at and near centers of GGθ, as indicated in figures 10 and 11, by "M" and "⌒" yielded the following information. In the Pacific area (figure 10) a majority of the GGθ maxima were located at least partially in covered (C) cloud areas. Of 18 such maxima 12 were entirely within and 6 partially within the covered cloud patterns. Another 15 maxima were distributed with 13 in MCO and 2 in MOP or O cloud areas. The Atlantic-European sectors have a distribution of GGθ maxima as follows: 17 in C (14 entirely and 3 partly), 2 in MCO and 8 in MOP or O. It appears that these maxima are most often associated with overcast conditions, however, there are also extensive regions of clouds where no relative GGθ maxima greater than .15 units occur.

Further inspection of figures 11A through 11E leads to the following miscellaneous observations. An extensive GGθ ridge spans the entirety of the northern edge of the Pacific area on 14, 15 and 17 December. This front lies very close to the mean winter position of the Pacific Arctic Front [11]. Apparently, a major air mass contrast is in this location although there is no well defined frontal cloud band. This is very likely due to the limit imposed by the satellite observations.

Looking further south, the angles between the GGθ fronts (ridges) and the cloud bands vary from right angles to near parallel, but an obvious relation exists between cloud bands and the ridges. The cloud pattern containing the vortex in the westernmost edge of the 13 December figure would definitely be in better relation to the GGθ front if the difference in time were considered. The reader is reminded that there is nearly four hours difference between the nephanalysis and GGθ analysis at this position.

The GGθ frontal analysis of 0000 GMT 14 December is difficult to relate to the cloud systems, except that the lack of occluded structure in GGθ is apparent. Frontal analyses on the succeeding three days in the Pacific area generally show reasonable relations to the cloud bands with 16 December being the outstanding example. It is noted on these same days that the GGθ fronts could be most readily associated with cloud bands when long trailing cloud bands were involved.

FNWF, working in conjunction with Project FAMOS, was subjectively, but selectively, introducing satellite data into the 1000 and 500-mb numerical analyses in the east Pacific area during the period of this study [2]. This was accomplished on an irregular basis as an input to the so-called update analyses for 00Z, which includes all data received for 00Z within the following 12 hours. Since the operational analyses were used in this study, the only consequence of this procedure is the effect of weather-satellite imposed continuity carried to the operational analysis for the following day. Information obtained from FNWF and Project FAMOS revealed that the only major input of satellite data during this period was 0000 GMT 12 December. The relative effect on 13 December and following dates is difficult to assess but appears to be of little consequence.

Figures 11A through 11E graphically relate the GGθ ridges and clouds in the Atlantic-European areas. The western portion of these figures is in the relatively dense data Atlantic Ocean area. In the ocean area at 1200 GMT 11 December, little association can be found between the GGθ fronts and cloud bands, except that the lack of depiction of the occluded system is apparent. The extensive cloudiness over the land mass additionally is difficult to relate to the GGθ ridges.

It should be noted, however, that these cloud patterns generally meet the definition of a mass rather than that of a cloud band. The 1200 GMT 12 December figure illustrates a good association between the GGθ fronts and cloud bands in the ocean area, except that there is no obvious association between the GGθ ridge and the NE-SW cloud band south of the cloud vortex. Once again, it is difficult to relate the extensive cloudiness over the land mass and the GGθ fronts; however, on the 1200 GMT 13 December illustration, the cloud patterns are better defined as bands and can be more easily related to the GGθ ridges. The GGθ front and cloud band relationship on the 1200 GMT 14 December illustration closely approximates the relations in figure 2, except that the GGθ analysis does not depict the occlusion. The weak baroclinic zone near 15-20N, discussed earlier, is evident on 1200 GMT 15 December as it was on the earlier days in the period.

In summary, it has been seen that only in some cases can the FNWF frontal analyses and nephanalyzed cloud bands be related as suggested by the model in figure 2. The model is approached more closely in the relatively dense-data Atlantic Ocean area compared to the Pacific area.

7. Vertical Motion versus Clouds and Frontal Analyses

a. Introduction

A logical extension of the preceding studies is an investigation of vertical motion and its relation to cloud patterns. FNWF computes vertical velocities at the 850-mb and 500-mb levels which represent vertical motion in the lower troposphere and upper troposphere, respectively [8]. Examples of these two analyses are shown in figures 12 and 13. The analyses are contoured at 1, 2, 4 and 8 cm sec^{-1} for

upward (+) motion but are not contoured for downward (-) motion. 850-mb and 500-mb analyses at 0000 GMT and 1200 GMT were chosen for comparison with satellite-observed nephanalyses within four hours of these times. The period selected for this study was the same as that of Phase II, just discussed, that is, 13-17 December in the Pacific areas and 11-15 December in the Atlantic-European areas.

b. Results

(1) 850-mb Study

The average amount of clouds in areas of ascent and descent at the 850-mb level was determined. Additionally, the average cloud amount in regions of vertical ascent greater than 1 cm sec^{-1} was evaluated. The results are tabulated in Tables 9 and 10 for the Pacific and Atlantic-European areas, respectively. The average percent of cloud cover, in categories of amounts C, MCO, and combined MOP and O, was determined separately for land and ocean areas. The values listed in Table 9 for the Pacific areas show that a higher portion of the areas of ascent contained MCO and C clouds than did the areas of descent: 65% versus 54% in the ocean area and 78% versus 53% in the land areas. The average amount of C and MCO cloud found in regions of ascent greater than 1 cm sec^{-1} rises to 88% in the ocean area but reduces to 74% over the land areas. Similar results were obtained in the Atlantic-European land and ocean areas with two notable exceptions. One, the average cloud amount in the ocean area of ascent (84%) was considerably larger than for the corresponding ocean area in the Pacific and, two, the correlation of percentage cloud cover and vertical motion is positive over land, negative over ocean. Also, for land areas the percent of C + MCO cover is relatively small, with 56% in ascent areas and 29% in descent areas.

In general, it was found that a greater average amount of clouds occur in regions of ascent that in regions of descent, the ratio being nearly 2 over land areas but only 1.5 over ocean regions. The correlation of percentage of cloud cover with vertical motion does not appear simple or necessarily positive.

(2) 500-mb Study

The 500-mb study was conducted in the same manner as the 850-mb study. The results are shown in Tables 11 and 12. Relative percentages are much the same as at 850-mb. Again there is a greater average amount of cloud cover in areas of ascent than in regions of descent (especially over land). Also, a more reasonable relation of cloud cover to magnitude of vertical motion is apparent.

(3) Graphical Relation of Clouds, Vertical Motion and GGθ Ridges

Figures 14 and 15 graphically relate the areas of ascent and descent, at the 850-mb and 500-mb levels, to the major cloud patterns. The 0 and 1 cm sec^{-1} contours are drawn in these figures for both levels. Additionally, the regions where the vertical velocity is greater than 1 cm sec^{-1} at either or both of the two levels have been shaded. The GGθ ridges are also included in these figures. An inspection of each of the figures reveals that in nearly all instances the 1 cm sec^{-1} contour at 850-mb was within the area bounded by the same isoline at 500-mb. This is statistically indicated by a comparison of the combined regions (i.e. w_{500} and/or w_{850} greater than 1 cm sec^{-1}), as shaded in figures 14 and 15, with the areas of w_{500} greater than 1 cm sec^{-1}. In the Atlantic-European area the combined regions were 7% larger overall than the similar area at 500 mb, while in the Pacific they were less than

5% larger. Therefore, it can be assumed for this study that the region of vertical motion greater than 1 cm sec^{-1} at 500 mb generally includes the similar region at the 850-mb level.

Examination of the major shaded areas in figures 14A through 14E shows that a considerable portion of such areas fell behind (i.e. on the cold air side) rather than ahead of the major covered cloud systems. Specifically, this occurred nine out of twelve times; three exceptions are noted, two in the westernmost portion of the Pacific on 16 and 17 December, and a third in the eastern Pacific on 13 December. The vertical ascent areas are also consistently on the cold side of the cloud systems in the Atlantic Ocean area (figure 15) on 11 through 13 December; however, on 14 and 15 December, the cloud systems were mainly within the region of greatest vertical ascent. In the land portion of the Atlantic-European areas, this latter relation was most often true. However, since MCO areas generally occur on the cold side of C areas (figures 10 and 11) the above statistics would show a more favorable cloud-vertical motion relation if the MCO areas were included in figures 14 and 15. Study of the vertical motion and cloud relationship in the Pacific area disclosed major cloud patterns in regions of strong descent at both levels (see figures 14A through 14E) as well as a small amount or no covered clouds in areas of strong ascent associated with numerically analyzed frontal systems. The vertical motion-cloud relation must, therefore, be regarded as suspect in sparse data areas.

In all instances, the major areas of maximum vertical ascent can be related to a numerical front with the majority of centers of maximum vertical ascent in zones of strong baroclinicity (30 centers in hyper-baroclinic zones versus 19 in quasi barotropic zones in the Pacific;

27 versus 13 in the Atlantic-European). This is in agreement with Sanders' model [15]. It was further noted that the GGθ maxima (indicated by "M" on figures 14 and 15) were frequently (24 of 40 times in the Pacific and 12 of 25 in the Atlantic-European area) located in the region of maximum ascent (w greater than 1 cm sec^{-1}).

Since the areas of 500-mb vertical velocity greater than 1 cm sec^{-1} appeared to have some relation to the major cloud patterns, (shown in figures 14 and 15) a further study was made of this relation. The results are reported in Table 13, and include all cloud coverage categories in the area of w_{500} greater than 1 cm sec^{-1}. These figures show that on all dates cloud (C + MCO) coverage was 75% or greater over ocean areas and, with one exception, 50% or greater over the land areas. However, the clouds in the region of vertical velocity greater than 1 cm sec^{-1} by no means represented all the clouds. The last column in Table 13 relates the amount of MCO and C clouds in this region to the total amount of MCO and C clouds present in the total area studied. It can be seen that this is a small percentage (from 2% to 23%) of the total.

Although the cloud-vertical motion relation as studied here is not always clearly defined, the regions of 500-mb ascent greater than 1 cm sec^{-1} show a good relation to the major C + MCO cloud patterns.

8. Conclusions

Baroclinic zones contain a greater average percentage of cloud cover than quasi barotropic zones. The typical cloud band lies as much in a quasi barotropic zone as in a baroclinic zone and the typical cloud mass is most often situated with a greater portion in a quasi barotropic zone. These statements may at first seem contradictory,

but when the relatively large size of quasi barotropic zones is taken into consideration it is not unreasonable to assume that the quasi barotropic zones contain as much or more of the total cloud cover than the baroclinic zones. Statistics on precipitating clouds may yield different information but this category was not studied here.

The relations between cloud bands and baroclinic or quasi barotropic zones are not sufficiently distinct to be of unqualified operational application. The Phase I and II discussions generally lead to the conclusion that the numerical frontal analysis of FNWF, by itself, is not a reliable locator of frontal cloud bands.

The vertical motion discussion leads to the conclusion that the relation between the FNWF 850-mb and 500-mb vertical motion analyses and the cloud systems is not always simple. Regions of ascent at both 850 mb and 500 mb contain a larger percentage of clouds than do regions of descent. Areas of 500-mb ascent greater than 1 cm sec^{-1} generally are associated with 75% or more of C + MCO over oceans but only 50% or more (with exceptions) over land.

These relations do have some operational application, that is, one could use areas of vertical motion greater than 1 cm sec^{-1} at 500 mb to locate the major cloud systems and, further, expect to find less significant frontal cloud bands at and on the warm side of the GGθ ridge where vertical motion is usually less than 1 cm sec^{-1}.

Finally, some additional comments based on this study are offered with regard to satellite-observed clouds, numerically analyzed fronts and vertical motion.

(1) The numerically analyzed front can be used as a first approximation to locate frontal bands but it is not sufficiently reliable for use as a cloud locator in sparse data areas and in occluded sections of the frontal zone.

(2) The numerically analyzed vertical motion fields, especially where 500-mb ascent exceeds 1 cm sec^{-1}, can be used to locate major cloud systems (C + MCO) with the shape of the system given by this isoline. This is probably the best application of the vertical motion analyses.

(3) Upon working with satellite-cloud data, in conjunction with analyses of baroclinicity, it becomes increasingly suggestive that some sort of digital input of satellite-cloud observations into the numerical analysis program would most certainly enhance the accuracy of baroclinicity. This would then make the latter more valuable for locating frontal bands in sparse data areas.

(4) Since the frontal and vertical motion analyses are basically dependent upon the same data input, any modifications such as mentioned in (3) above would also be effective in improving the vertical motion analyses.

BIBLIOGRAPHY

1. Anderson, R. K., E. W. Ferguson, and V. J. Oliver, The Use of Satellite Pictures in Weather Analysis and Forecasting. World Meteorological Organization, Geneva, Switzerland, Technical Note No. 75, 1966: 184 pages.

2. Arnold, W.S.M. and W. D. Groscup, Use of Data in Fleet Numerical Weather Facility Products as Derived from Meteorological Satellites. Paper read at the 47th annual AMS meeting, New York City, January 23-26, 1967. (Abstract, Bulletin of the AMS, v. 47, November 1966: 900).

3. Berry, F. A. Jr., E. Bollay, and N. R. Beers, Handbook of Meteorology. McGraw-Hill, 1945: 1068 pages.

4. Boucher, R. J. and R. N. Newcomb, Synoptic Interpretation of Some TIROS Vortex Patterns: A Preliminary Cyclone Model. Journal of Applied Meteorology, v. 1, June 1962: 127-135.

5. Dickson, R. R. The Weather and Circulation of December 1966. Monthly Weather Review, v. 95, March 1967: 148-152.

6. Dryden, V. D. Hemispheric Frequency and Intensity of Numerically Analyzed Baroclinic Zones. Unpublished paper, Department of Meteorology and Oceanography, Naval Postgraduate School, Monterey, California, September 1966: 20 pages.

7. Hadfield, R. G., E. J. Wiegman, W. Viezee, and S. M. Serebreny, Meteorological Interpretation of Satellite Cloud Photographs. Stanford Research Institute, Menlo Park, California. Final Report (Contract CWB 10481). January 1964: 159 pages.

8. Hughes, R. E. Computer Products Manual. Fleet Numerical Weather Facility, Monterey, California, Technical Note No. 21, July 1966: 310 pages.

9. Krishnamurti, T. N., J. Nogues, and D. Baumhefner. On the Partitioning of the Baroclinic Vertical Motions in a Developing Wave Cyclone. Department of Meteorology, University of California, Los Angeles, California. Scientific Report No. 1 (Contract No. AF19(628)-4777, Project No. 6698, Task No. 669802). May 1966: 33 pages.

10. McCord, H. E. Jr., Relationship Between Satellite-Observed Cloud Phenomena and Numerically Analyzed Baroclinic Zones. Unpublished manuscript, Department of Meteorology and Oceanography, Naval Postgraduate School, Monterey, California, October 1966: 29 pages.

11. Petterssen, S. Introduction to Meteorology, 2nd Edition. McGraw-Hill, 1958: 327 pages.

12. Petterssen, S. Weather Analysis and Forecasting, Volume II, Weather and Weather Systems. McGraw-Hill, 1956: 428 pages.

13. Renard, R. J. and L. C. Clarke, Experiments in Numerical Objective Frontal Analysis. Monthly Weather Review, v. 93, September 1965: 548-556.

14. Sanders, F. Further Research Directed Toward the Study of Relations of Atmospheric Flow to Weather. Department of Meteorology, Massachusetts Institute of Technology, Cambridge, Massachusetts. Final Report (Contract No. AF19(604)-8373, Project No. 8641, Task No. 86410). July 1963: 159 pages.

15. Shoemyer, J. W. and J. B. Tupaz. A Study of the Relationship Between the FNWF Frontal Analysis, Baroclinic and Barotropic Zones and the Satellite-Observed Nephanalysis Cloud Bands. Unpublished paper, Department of Meteorology and Oceanography, Naval Postgraduate School, Monterey, California. September 1966: 15 pages.

16. _____, Meteorological Satellite Observations. Project FAMOS, U. S. Fleet Weather Central, Washington, D.C. Field Memorandum (Revised), July 1966.

APPENDIX I

Definitions of Weather Satellite Terminology [16]

Cloud Amount (Coverage)

O - - - - -	Open - - - - - - - - - - - - - - -	less than 20%
MOP - - - -	Mostly Open - - - - - - - - - - -	20% - 50%
MCO - - - -	Mostly Covered - - - - - - - - - -	51% - 80%
C - - - - -	Covered - - - - - - - - - - - - -	greater than 80%

Cloud Mass

A large-scale area of reflection from clouds, with covered (C) conditions unless otherwise specified.

Cloud Pattern

An arrangement or distribution of cloud elements, distinct groups of cloud elements, or cloud masses which show a distinctive organization. Cloud patterns of all scales appear in satellite photographs. The distinctive cloud pattern produced by mountain waves is a mesoscale pattern, while a cloud VORTEX is a macroscale pattern.

Cloud System

The cloudiness produced by or associated with a specific type of atmospheric system. Examples of atmospheric systems which produce distinctive cloud patterns are occluding cyclones, cold upper air lows, tropical storms, etc.

Cloud Band

A synoptic scale, solid, covered (C), or mostly covered (MCO) cloud pattern which has a width of at least 1° lat (60 n mi), and a length-to-width ratio of at least 4:1. CLOUD BANDS are usually curved.

Frontal Band

A CLOUD BAND in the mid-latitudes which is believed to be associated with a surface front.

Vortex

A pattern with one major CLOUD BAND spiraling into a center, indicating a definite center of circulation, that is, at least one closed contour for at least one level in conventional analyses. Circulations which have been cold-core for some time have a short band extending in toward the center, while warm-core circulations have a long FRONTAL BAND.

PVA MAX

A covered (C), bright, isolated, comma-shaped pattern composed of middle or high clouds, 3^{o} lat (180 n mi) or more in length, usually observed in the south or west sector of a cyclone. This distinctive pattern normally represents an area of maximum advection of positive relative vorticity. It usually precedes a short-wave trough at 500 mb.

Major

Cloud pattern or system bounded by  on NMC nephanalysis.

TABLE 1

LATITUDE BAND	AVG GGθ C/(100km)^2		PERCENT OF LATITUDE BAND IN:		PERCENT OF BAROCLINIC ZONES WITH CLOUD AMT:			PERCENT OF QUASI BAROTROPIC ZONES WITH CLOUD AMT:		
	Ridges	Troughs	Baro-clinic zone	Quasi baro-tropic zone	C	MCO	Total	C	MCO	Total
15° to 30°N	.11	-.05	24%	76%	30%	16%	46%	11%	8%	19%
30° to 45°N	.17	-.13	37%	63%	51%	26%	77%	25%	16%	41%
45° to 60°N	.20	-.15	33%	67%	63%	15%	78%	38%	14%	52%
	AREA AVERAGE		30%	70%	41%	20%	61%	19%	11%	30%

TABLE 2

LATITUDE BAND	AVG GGθ C/(100km)^2		PERCENT OF LATITUDE BAND IN:		PERCENT OF BAROCLINIC ZONES WITH CLOUD AMT:			PERCENT OF QUASI BAROTROPIC ZONES WITH CLOUD AMT:		
	Ridges	Troughs	Baro clinic zone	Quasi baro-tropic zone	C	MCO	Total	C	MCO	Total
15° to 30°N	.11	-.08	39%	61%	13%	12%	25%	8%	12%	20%
30° to 45°N	.19	-.09	30%	70%	41%	18%	59%	19%	15%	34%
45° to 60°N	.20	-.19	37%	63%	65%	9%	74%	30%	7%	37%
	AREA AVERAGE		37%	63%	31%	13%	44%	16%	12%	28%

TABLE 3

AREA	TYPE CLOUD BAND AND COVERAGE	CASES	AVG ANGLE BETWEEN GGθ RIDGE AND BAND	RANGE OF ANGLES	AVG GGθ $\left[C/(100km)^2\right]$ VALUE IN RIDGE	% CLOUD BAND IN	
						BAROCLINIC ZONE	QUASI BAROTROPIC ZONE
E	Frontal Covered	18	29°	10° to 90°	.17	55%	45%
	Non-frontal Covered	9	15°	5° to 45°	.13	35%	65%
	Non-frontal Mostly Covered	8	8°	0 to 10°	.09	33%	67%
F	Frontal Covered	1	90°		.20	40%	60%
	Non-frontal Covered	0					
	Non-frontal Mostly Covered	0					

TABLE 4

AREA	TYPE CLOUD MASS AND COVERAGE	CASES	AVG GGθ [C/(100km)^2] VALUE IN RIDGE	PERCENT CLOUD MASS IN	
				BAROCLINIC ZONE	QUASI BAROTROPIC ZONE
E	Frontal Covered	12	.17	46%	54%
	Non-frontal Covered	38	.14	48%	52%
	Non-frontal Mostly Covered	31	.11	41%	59%
F	Frontal Covered	1	.16	50%	50%
	Non-frontal Covered	6	.18	68%	32%
	Non-frontal Mostly covered	1	.15	30%	70%

TABLE 5

AREA	TYPE CLOUD BAND AND COVERAGE	CASES	AVG ANGLE BETWEEN GGθ RIDGE AND BAND	RANGE OF ANGLES	AVG GGθ $[C/(100km)^2]$ VALUE IN RIDGE	% CLOUD BAND IN	
						BAROCLINIC ZONE	QUASI BAROTROPIC ZONE
A	Frontal Covered	8	14°	5° to 35°	.25	61%	39%
	Non-frontal Covered	10	29°	0 to 90°	.16	51%	49%
	Non-frontal Mostly Covered	1	10°		.07	50%	50%
B	Frontal Covered	2	12°	10° to 15°	.12	78%	22%
	Non-frontal Covered	7	13°	0 to 30°	.16	63%	37%
	Non-frontal Mostly Covered	0					
C	Frontal Covered	0					
	Non-frontal Covered	10	28°	0 to 90°	.23	55%	45%
	Non-frontal Mostly Covered	2	12°	10° to 15°	.15	20%	80%
D	Frontal Covered	0					
	Non-frontal Covered	0					
	Non-frontal Mostly Covered	12	Indefinite		.11	50%	50%

TABLE 6

AREA	TYPE CLOUD MASS AND COVERAGE	CASES	AVG $GG\theta$ $[C/(100km)^2]$ VALUE IN RIDGE	PERCENT CLOUD MASS IN	
				BAROCLINIC ZONE	QUASI BAROTROPIC ZONE
A	Frontal Covered	0			
	Non-frontal Covered	12	.16	46%	54%
	Non-frontal Mostly Covered	13	.14	28%	72%
B	Frontal Covered	0			
	Non-frontal Covered	20	.16	44%	56%
	Non-frontal Mostly Covered	5	.15	43%	57%
C	Frontal Covered	0			
	Non-frontal Covered	7	.15	76%	24%
	Non-frontal Mostly Covered	4	.20	50%	50%
D	Frontal Covered	0			
	Non-frontal Covered	28	.11	42%	58%
	Non-frontal Mostly Covered	12	.12	55%	45%

TABLE 7

CASES	AVG GGθ $[C/(100km)^2]$ VALUE IN RIDGE	AVG LENGTH OF GGθ RIDGE	AVG CLOUD AMOUNTS IN					
			BAROCLINIC ZONE			BAROTROPIC ZONE		
			C	MCO	Total	C	MCO	Total
21	.29	43° LAT	51%	24%	75%	46%	15%	61%

TABLE 8

CASES	AVG GGθ $[C/(100km)^2]$ VALUE IN RIDGE	AVG LENGTH OF GGθ RIDGE	AVG CLOUD AMOUNTS IN					
			BAROCLINIC ZONE			BAROTROPIC ZONE		
			C	MCO	Total	C	MCO	Total
21	.25	55° LAT	43%	11%	54%	36%	11%	47%

TABLE 9

AREA	VERTICAL VELOCITY	AVG % OF CLOUD COVERAGE OF AMOUNTS:			
		C	MCO	C + MCO	MOP + O
OCEAN	> 0	45%	20%	65%	35%
LAND	> 0	78%	0%	78%	22%
OCEAN	< 0	22%	32%	54%	46%
LAND	< 0	42%	11%	53%	47%
OCEAN	> 1 cm/sec	74%	14%	88%	12%
LAND	> 1 cm/sec	74%	0%	74%	26%

TABLE 10

AREA	VERTICAL VELOCITY	AVG % OF CLOUD COVERAGE OF AMOUNTS:			
		C	MCO	C + MCO	MOP + O
OCEAN	> 0	55%	29%	84%	16%
LAND	> 0	44%	12%	56%	44%
OCEAN	< 0	23%	32%	55%	45%
LAND	< 0	19%	10%	29%	71%
OCEAN	> 1 cm/sec	75%	4%	79%	21%
LAND	> 1 cm/sec	63%	20%	83%	17%

TABLE 11

AREA	VERTICAL VELOCITY	AVG % OF CLOUD COVERAGE OF AMOUNTS:			
		C	MCO	C + MCO	MOP + O
OCEAN	> 0	45%	19%	64%	36%
LAND	> 0	79%	0%	79%	21%
OCEAN	< 0	23%	32%	55%	45%
LAND	< 0	35%	13%	48%	52%
OCEAN	> 1 cm/sec	58%	18%	76%	24%
LAND	> 1 cm/sec	80%	0%	80%	20%

TABLE 12

AREA	VERTICAL VELOCITY	AVG % OF CLOUD COVERAGE OF AMOUNTS:			
		C	MCO	C + MCO	MOP + O
OCEAN	> 0	52%	26%	78%	22%
LAND	> 0	44%	11%	55%	45%
OCEAN	< 0	28%	30%	58%	42%
LAND	< 0	13%	11%	24%	76%
OCEAN	> 1 cm/sec	69%	24%	93%	7%
LAND	> 1 cm/sec	55%	15%	70%	30%

TABLE 13

PACIFIC AREAS

AREA	DEC 66 DAY/GMT	AVG % OF CLOUD COVERAGE IN AMT				RATIO OF MCO + C IN "> 1cm/sec" AREA TO TOTAL MCO + C
		C	MCO	C + MCO	MOP + O	
OCEAN	13/00	73%	5%	78%	22%	.13
LAND	13/00	100%	0	100%	0	.10
OCEAN	14/00	61%	20%	81%	19%	.12
LAND	14/00	100%	0	100%	0	.19
OCEAN	15/00	56%	19%	75%	25%	.18
LAND	15/00	33%	0	33%	67%	.02
OCEAN	16/00	56%	20%	76%	24%	.12
LAND	16/00	50%	0	50%	50%	.04
OCEAN	17/00	49%	27%	76%	24%	.15
LAND	17/00	0	0	0	0	

ATLANTIC-EUROPEAN AREAS

OCEAN	11/12	80%	20%	100%	0	.10
LAND	11/12	62%	10%	72%	28%	.07
OCEAN	12/12	61%	25%	86%	14%	.21
LAND	12/12	69%	31%	100%	0	.09
OCEAN	13/12	72%	22%	94%	6%	.11
LAND	13/12	44%	16%	60%	40%	.08
OCEAN	14/12	69%	20%	89%	11%	.23
LAND	14/12	57%	13%	70%	30%	.09
OCEAN	15/12	70%	30%	100%	0	.23
LAND	15/12	50%	8%	58%	42%	.10

FIGURE 1

WARM SECTOR CLOUDS
RIDGE LINE
JET STREAK
OPEN CELLULAR
CLOSED CELLULAR
SURFACE
ACTIVE
INACTIVE

FIGURE 2

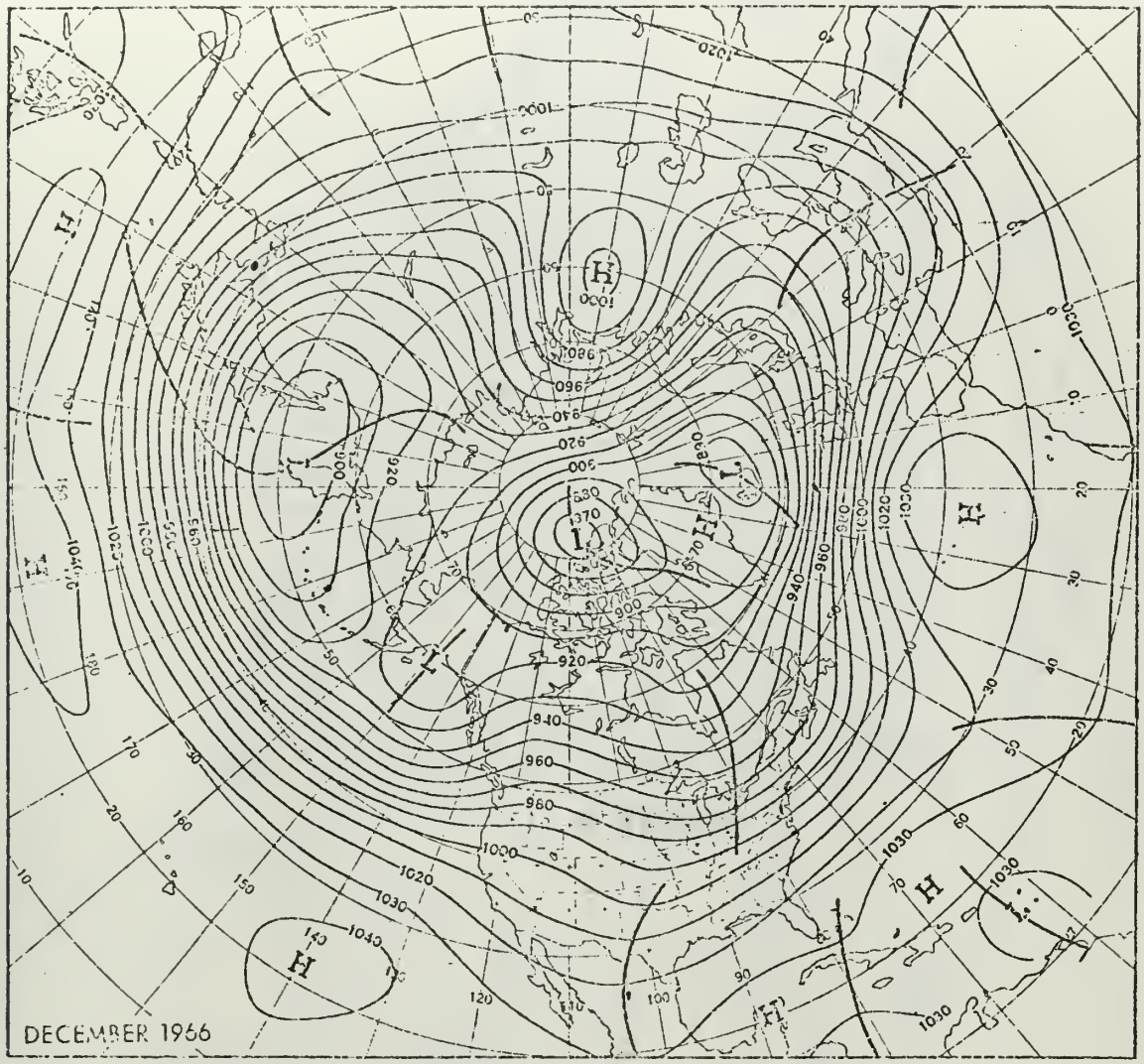

FIGURE 3

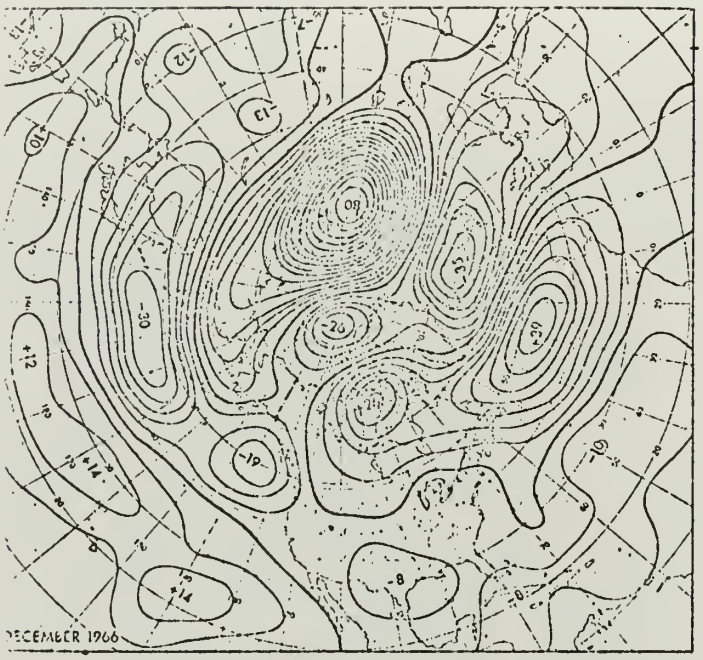

FIGURE 4

FIGURE 5

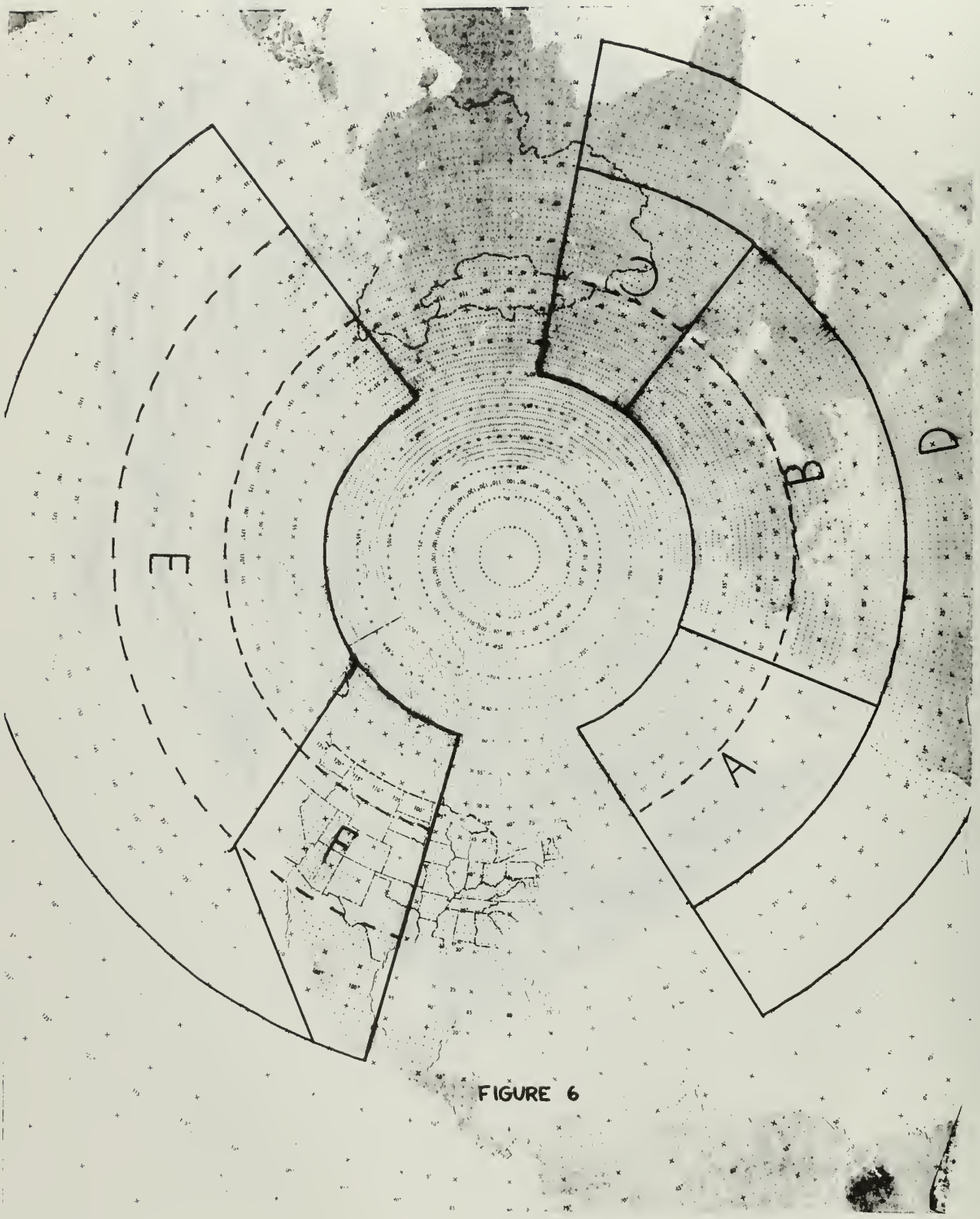

FIGURE 6

FIGURE 7

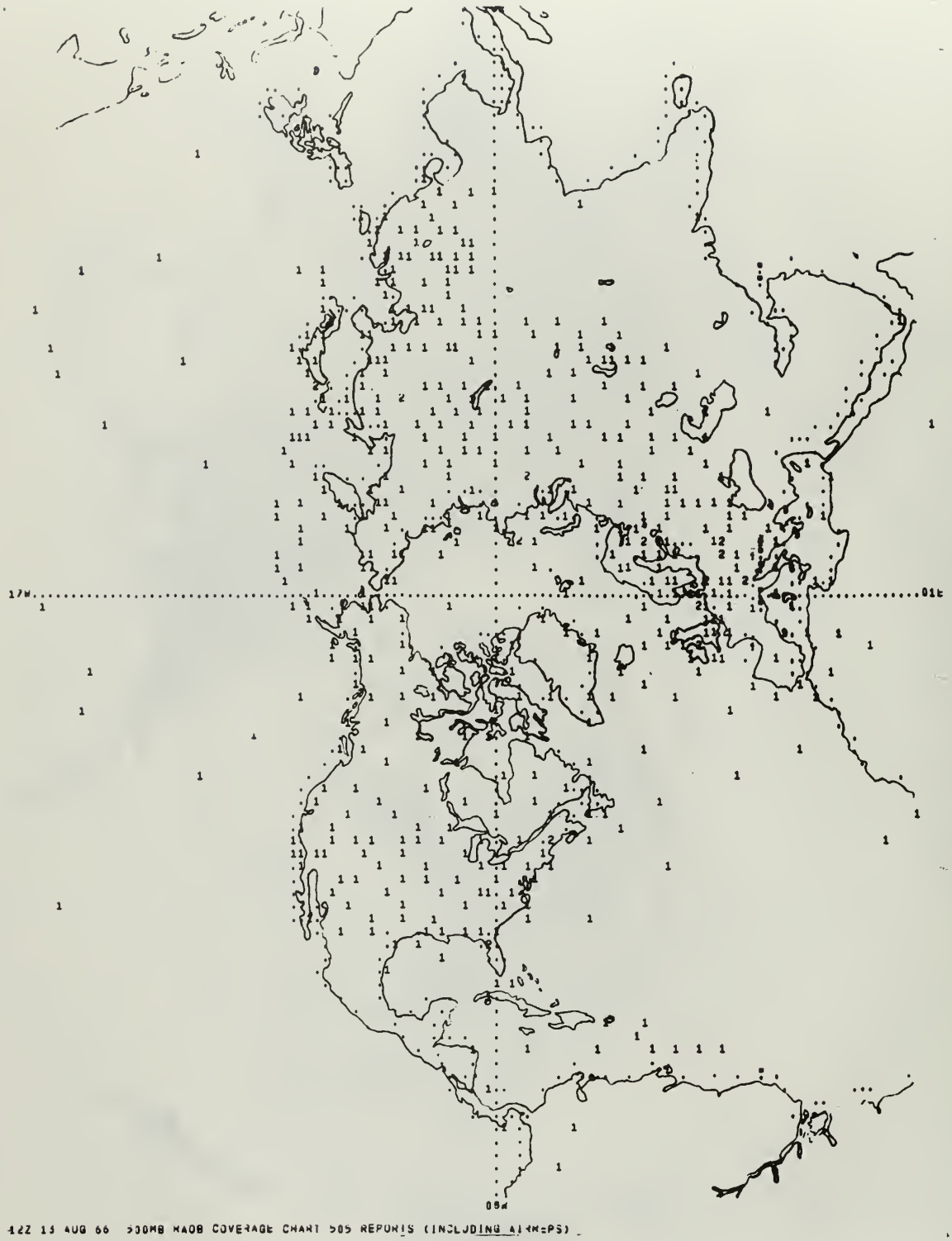
17W
01E
09W
422 15 AUG 66 500MB RAOB COVERAGE CHART 505 REPORTS (INCLUDING AIREPS)

FIGURE 8

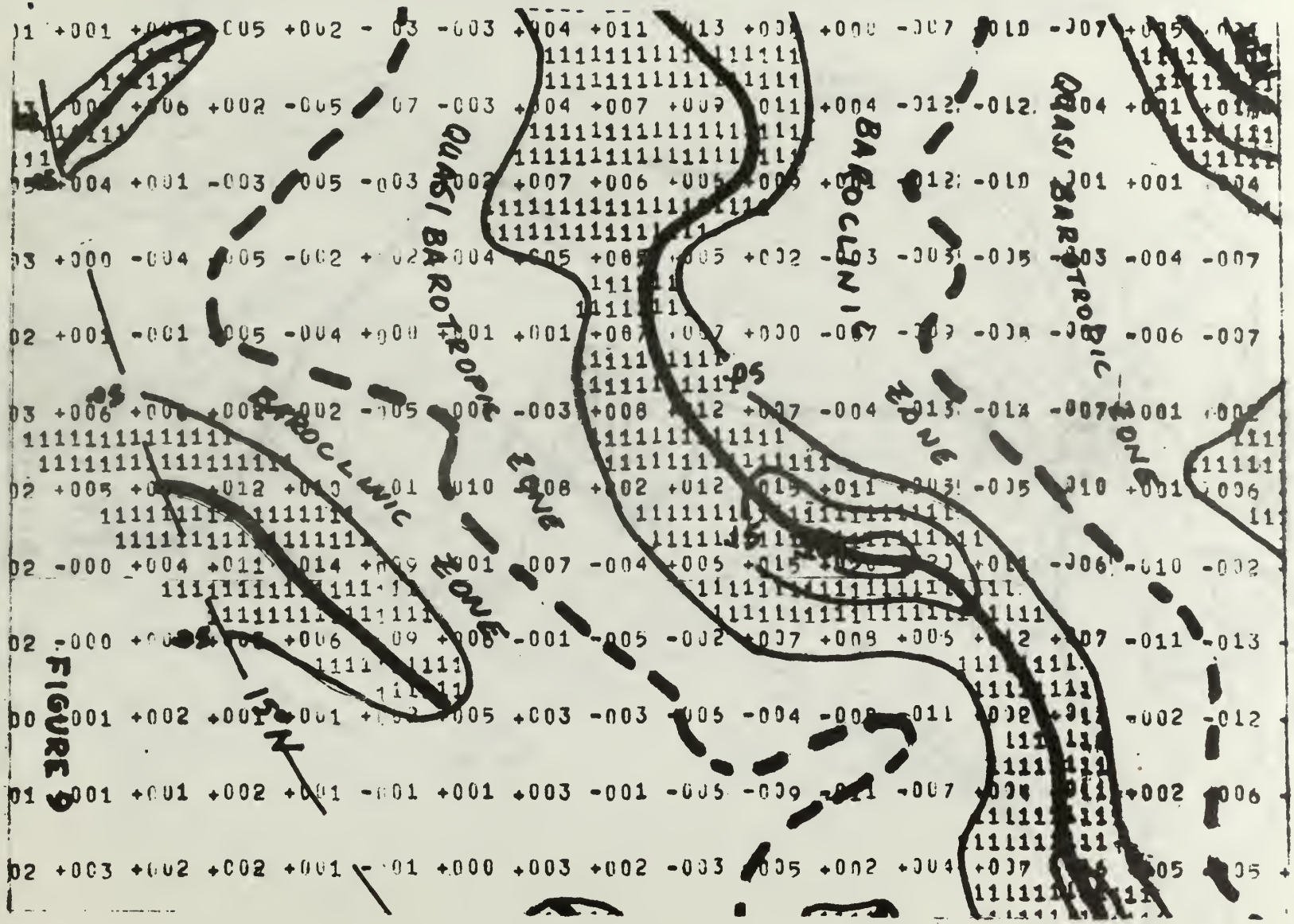
QUASI BAROTROPIC ZONE
BAROCLINIC ZONE
QUASI BAROTROPIC ZONE
BAROCLINIC ZONE
ISLAND

FIGURE 9

FIGURE 10A

FIGURE 10B

FIGURE 10C

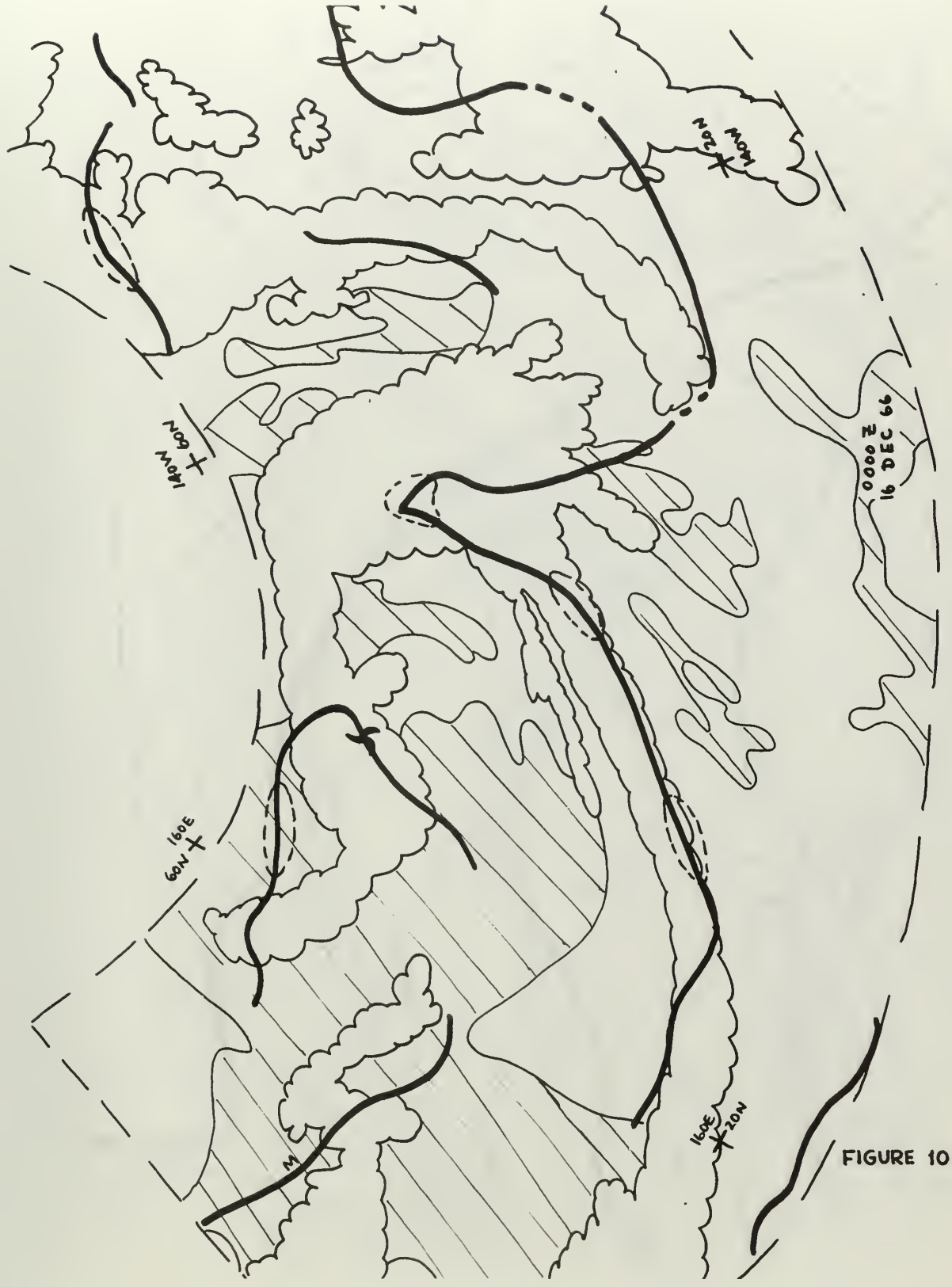

FIGURE 10D

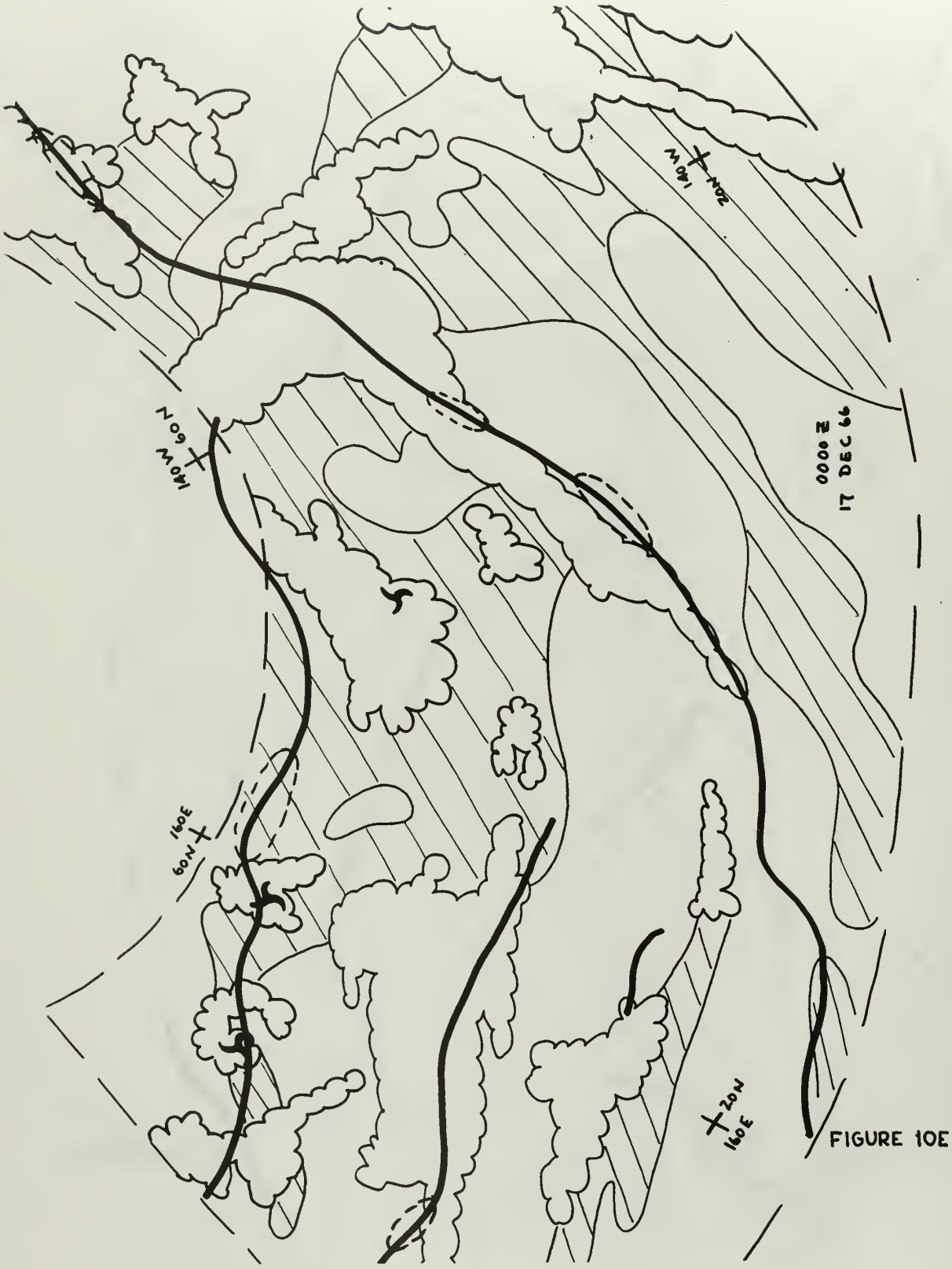

FIGURE 10E

FIGURE 11A

FIGURE 11B

FIGURE 11C

FIGURE 11D

FIGURE 11E

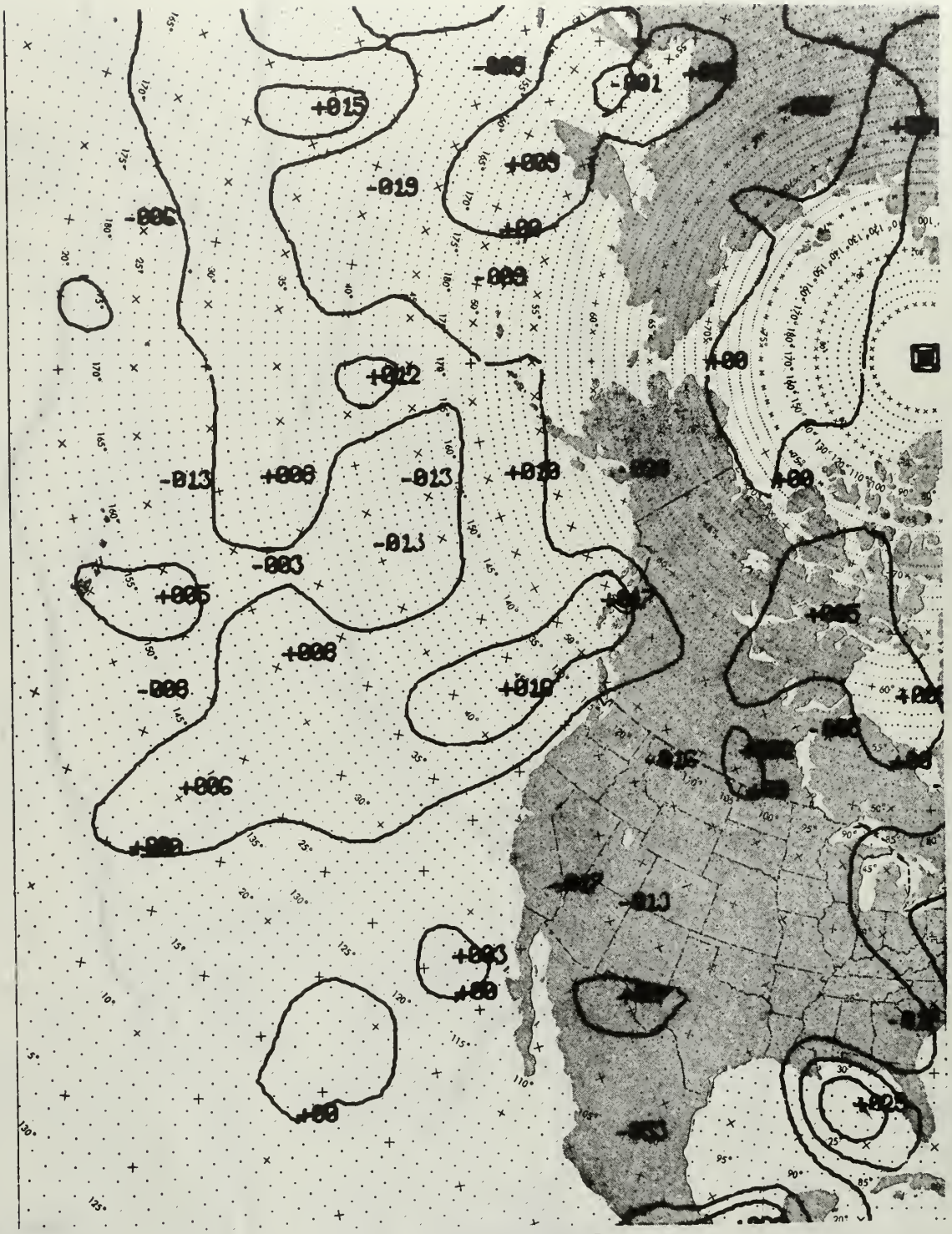

FIGURE 12

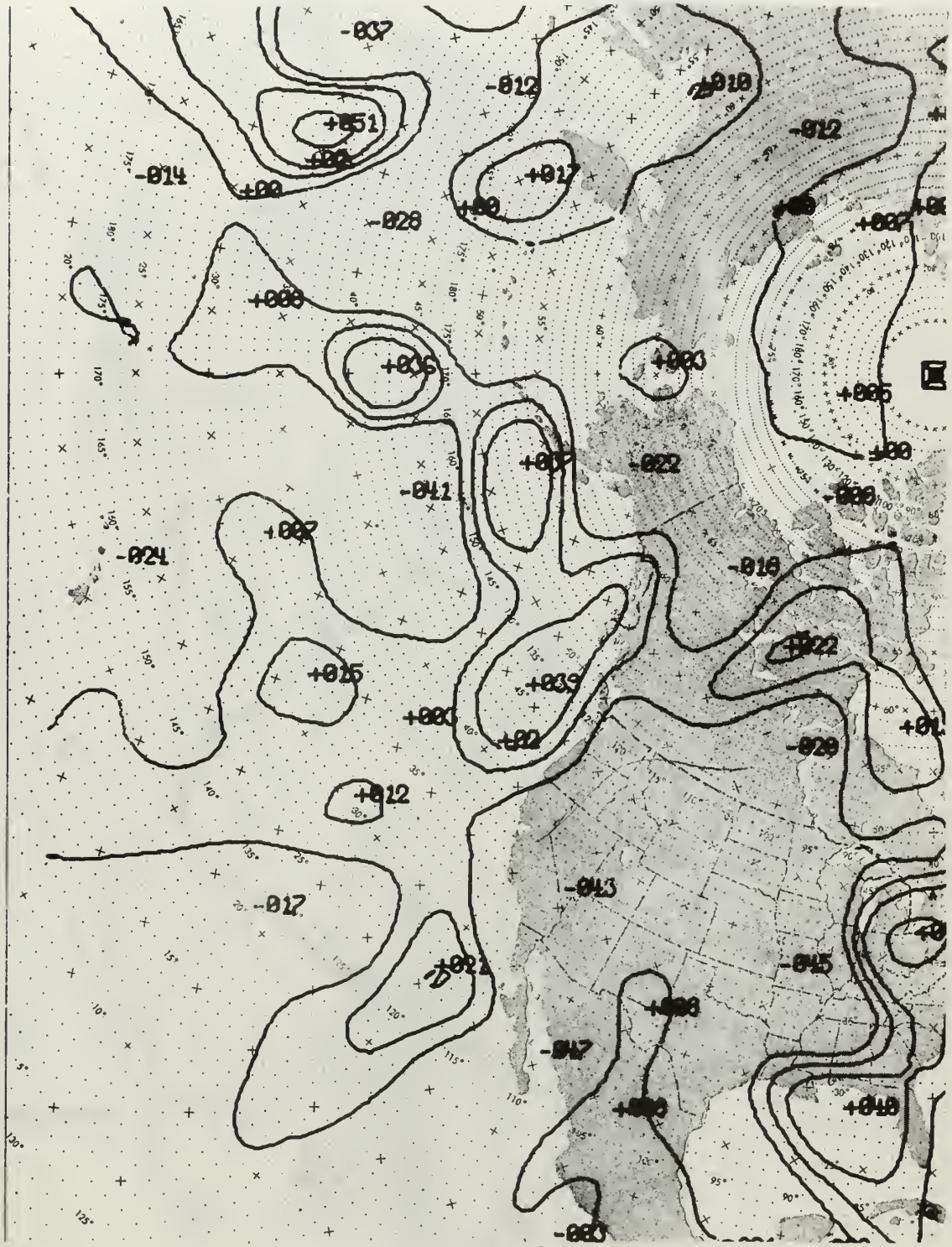
-037
-012
-010
-012
+051
-014
+017
-028
+036
+035
-022
-041
-024
-018
+022
+025
+039
+012
-029
-017
-043
-045
-047
+048

FIGURE 13

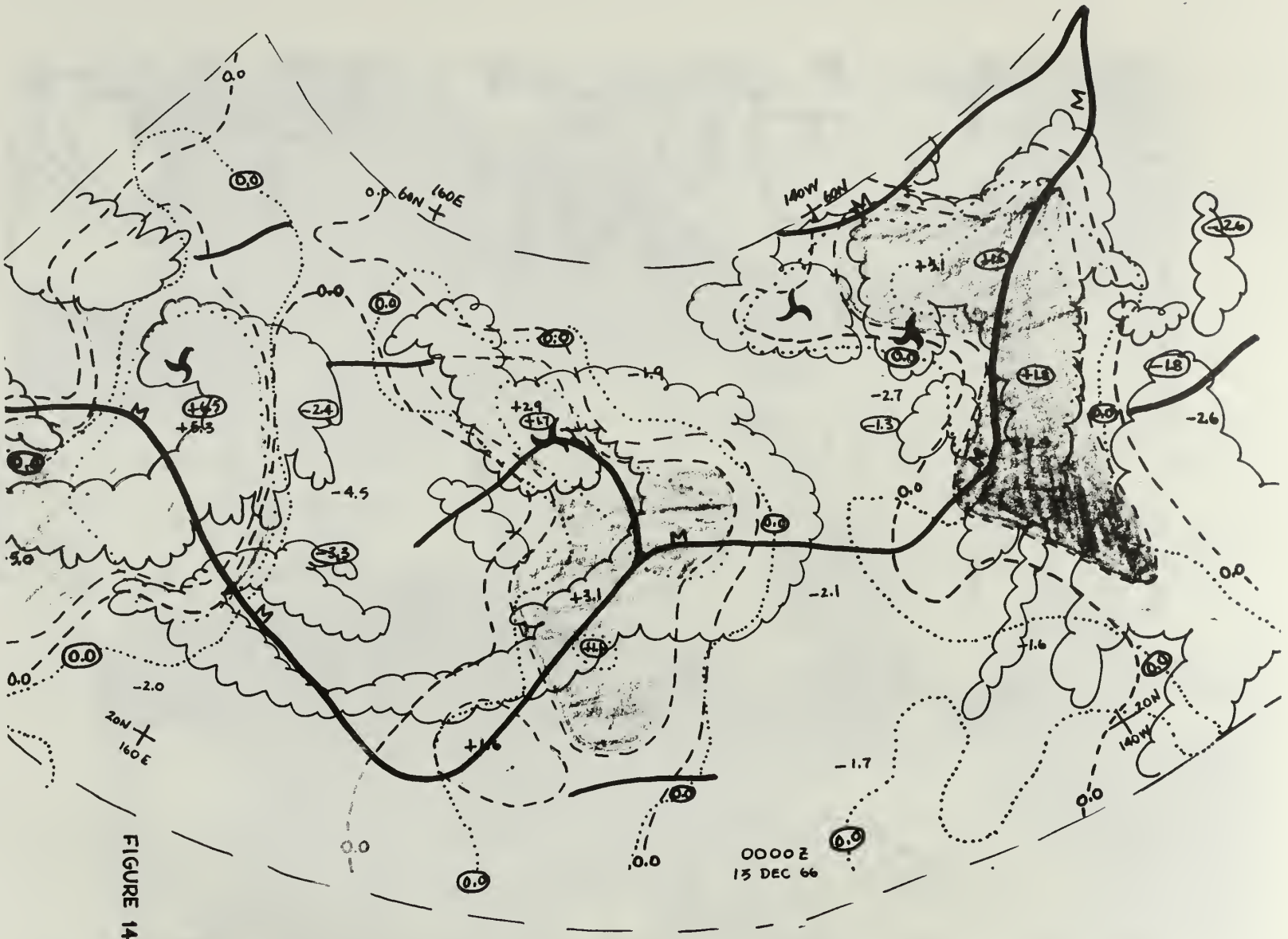
0.0
0.0
0.0 60N 160E
140W 60N
M
+2.1
+2.6
-2.6
0.0
0.0
0.0
-1.9
+2.9
+1.7
-2.7
-1.3
+1.8
-1.8
-2.6
+4.5
+6.3
-2.4
0.0
0.0
-4.5
0.0
-3.5
5.0
+3.1
-2.1
0.0
0.0
-2.0
1.6
0.0
20N 160E
20N 140W
-1.7
0.0
0.0
0.0
0.0
0.0
0000Z
13 DEC 66

FIGURE 14A

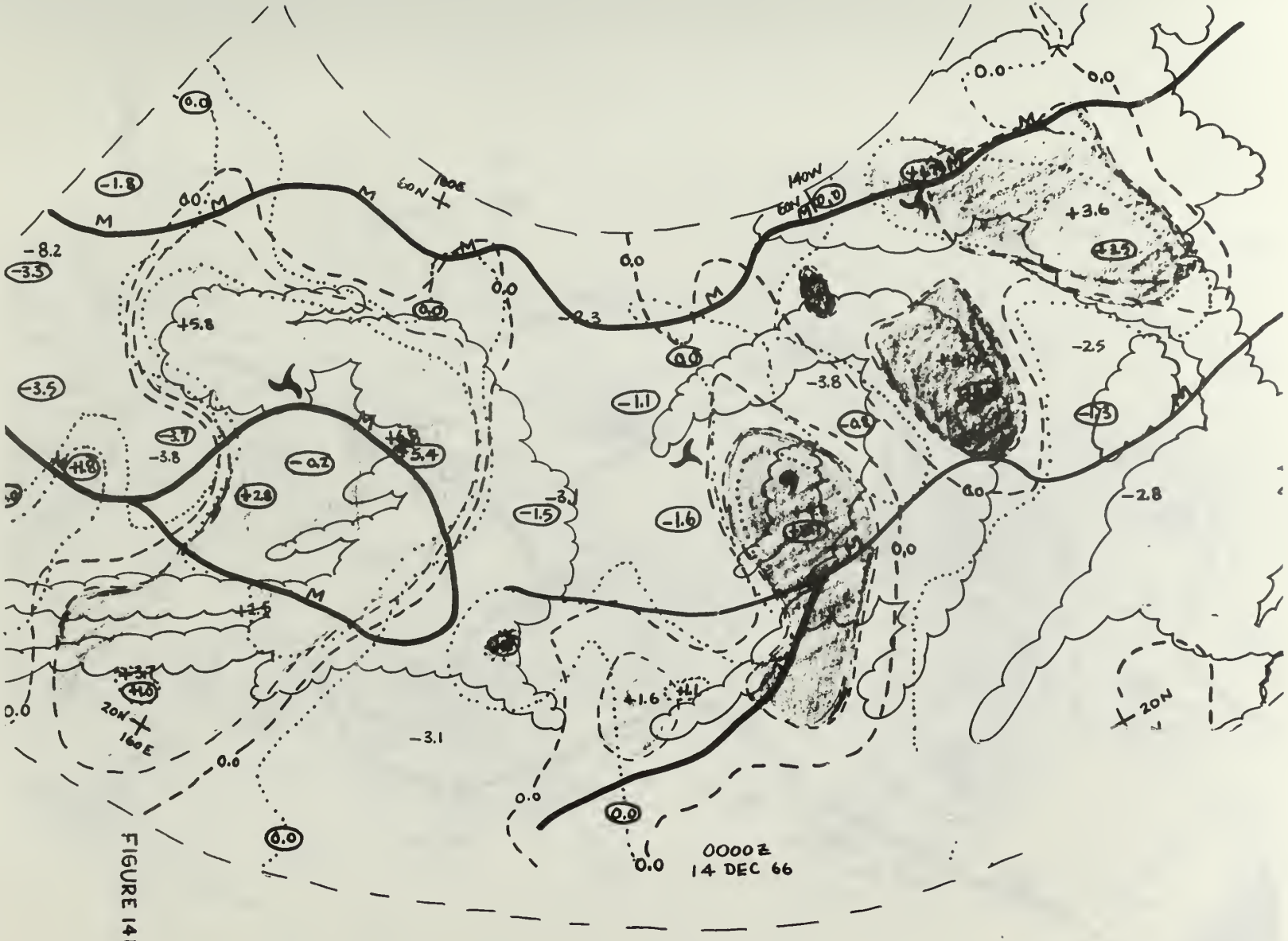

FIGURE 14B

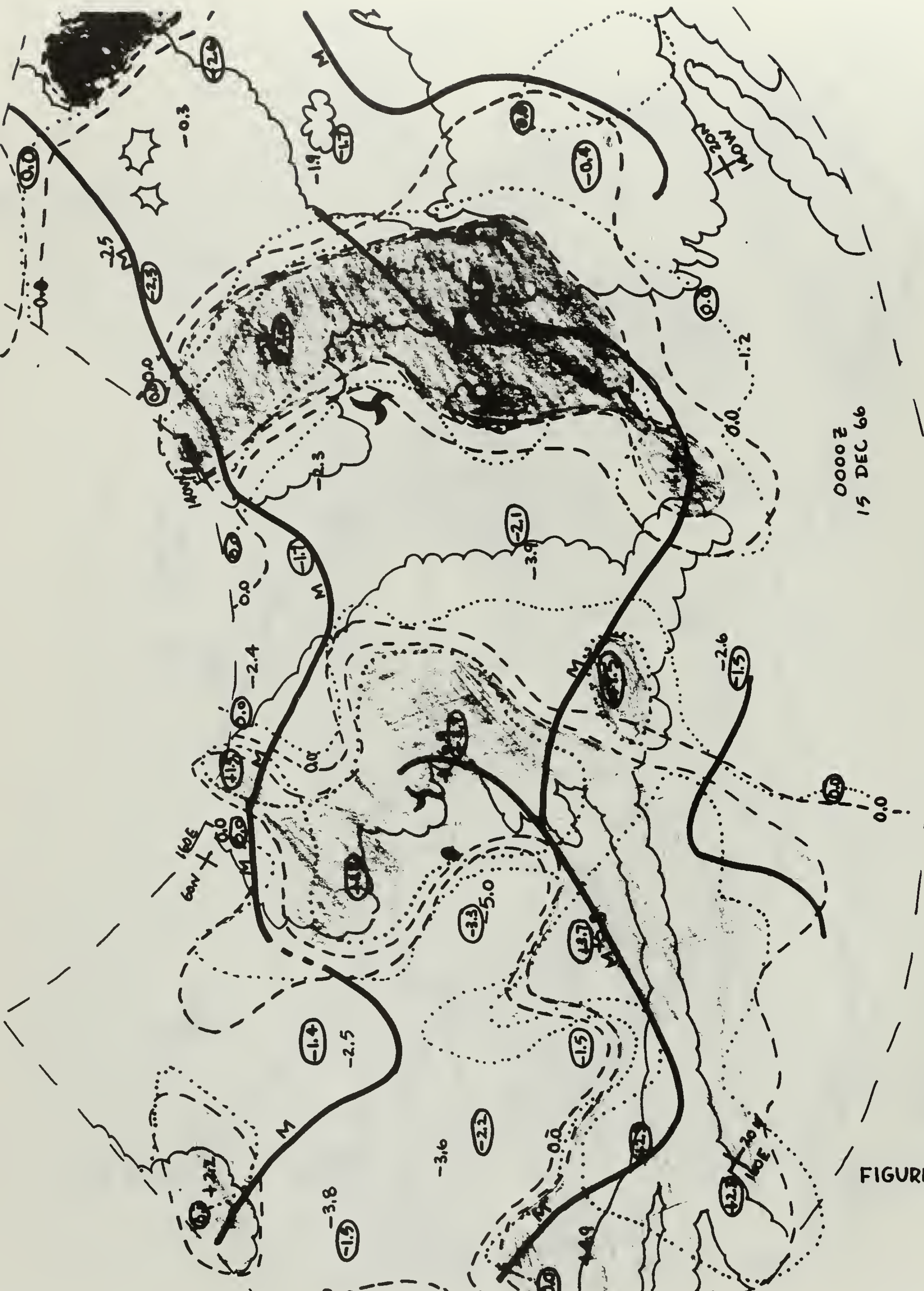

FIGURE 14C

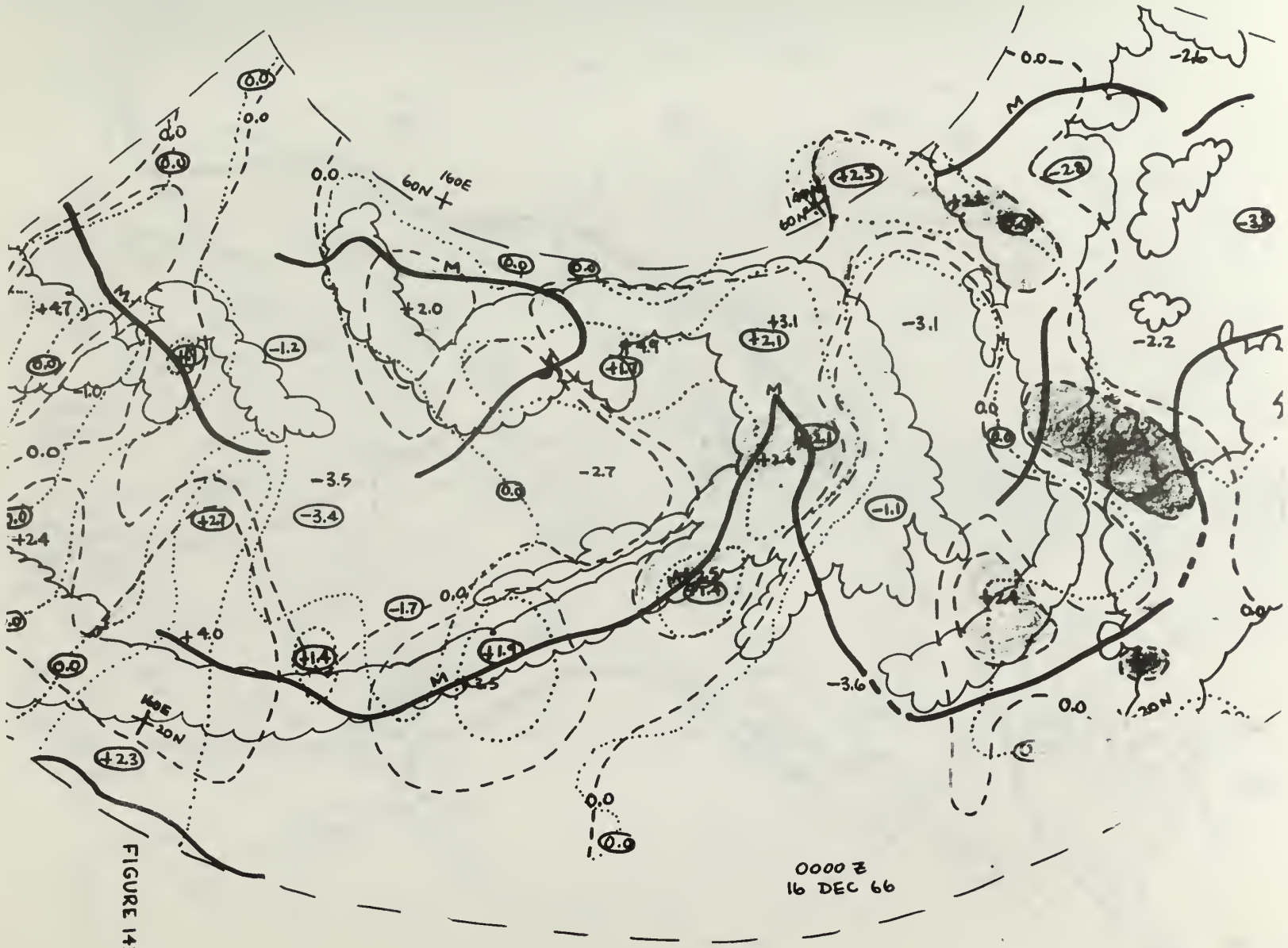

FIGURE 14D

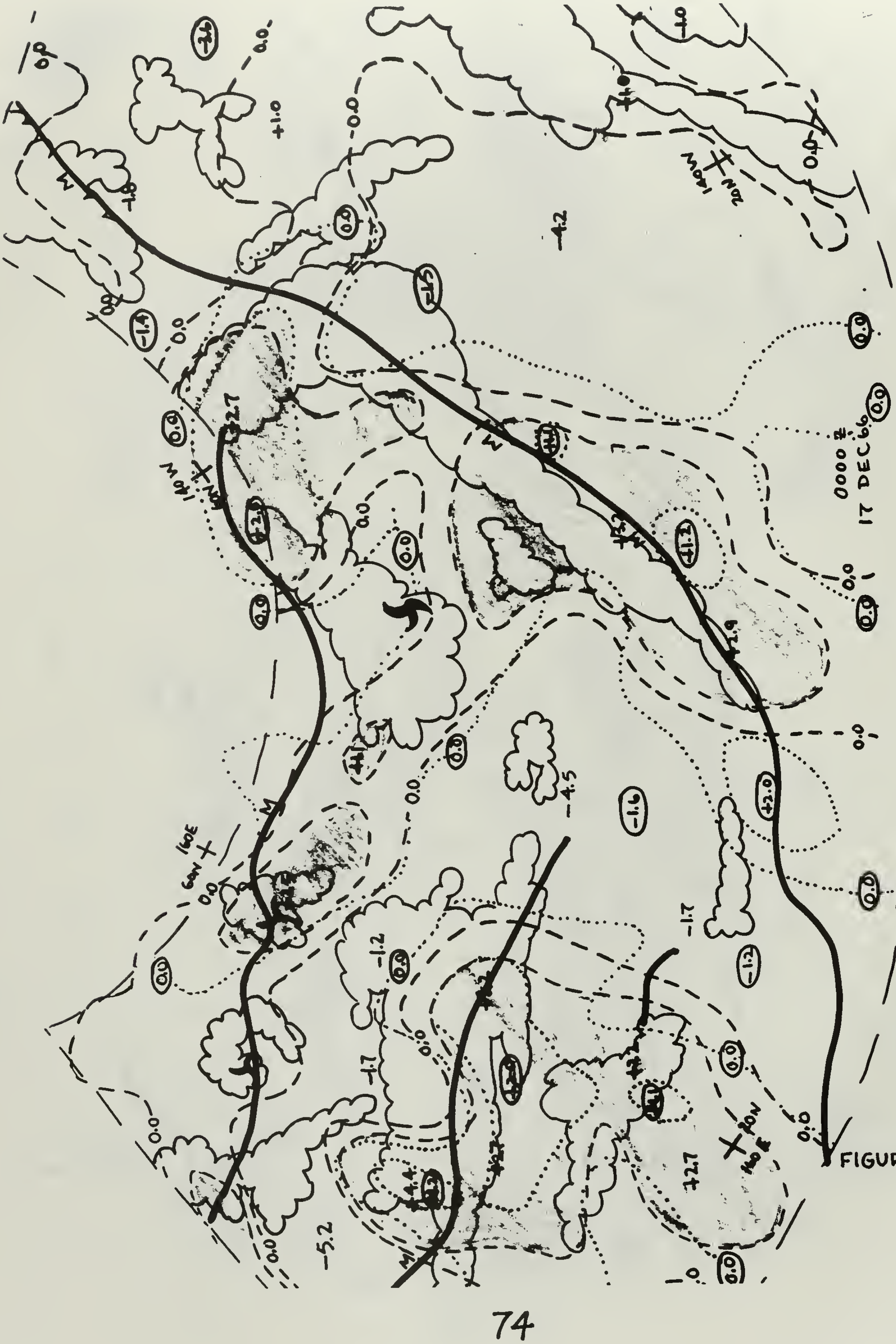

FIGURE 14E


0.0
-2.1
20W
60N
40E
60N
+1.4
M
-1.6
-1.6
0.0
0.0
+1.6
0.0
+1.2
-1.9
+1.4
0.0
0.0
+1.6
0.0
-1.5
-2.6
-1.0
0.0
0.0
-4.4
0.0
0.0
-2.4
-1.4
0.0
0.0
20N
20W
20N
40E
0.0
1200 Z
11 DEC 66

FIGURE 15A

FIGURE 15B

FIGURE 15C

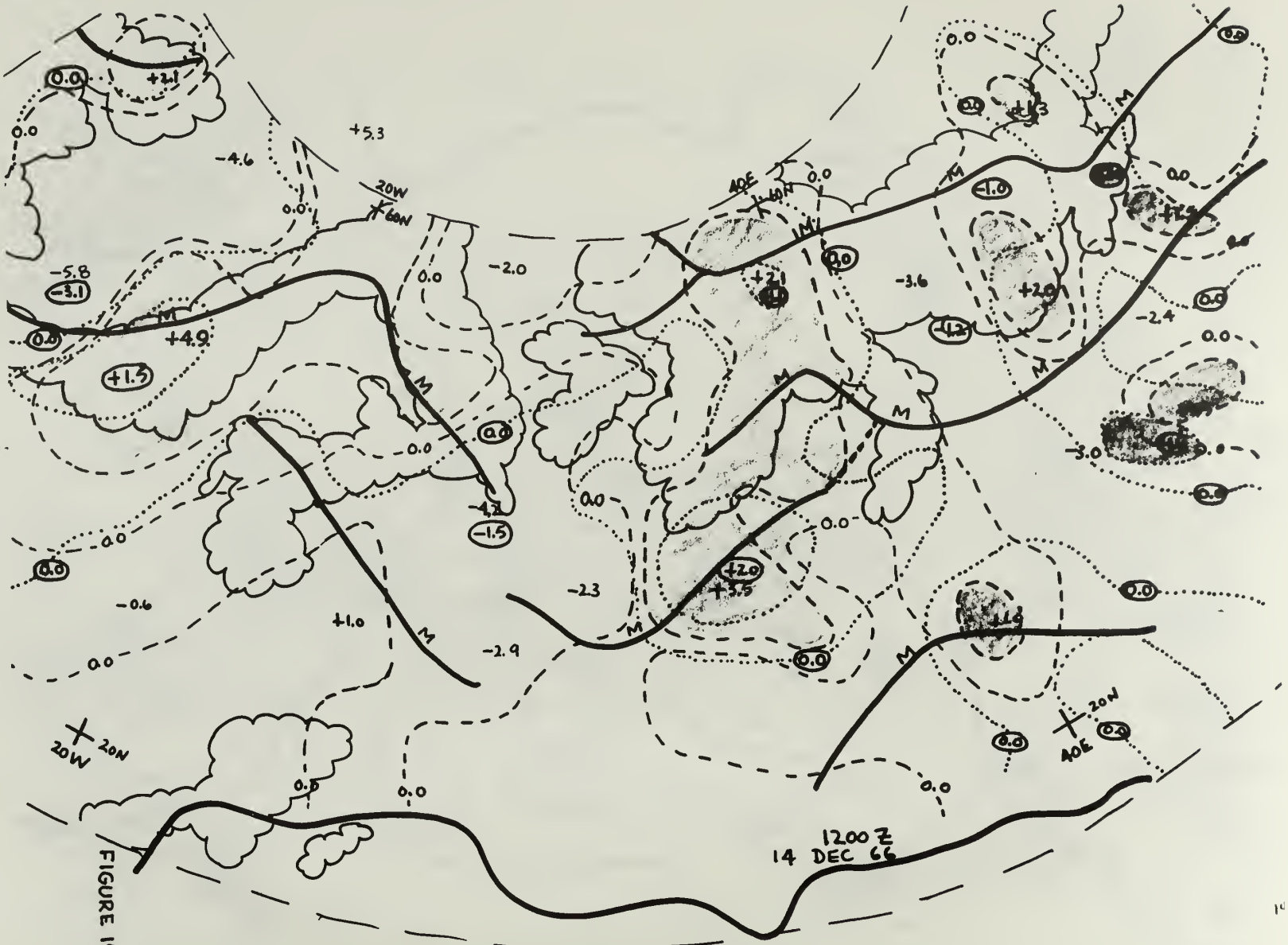

FIGURE 15D

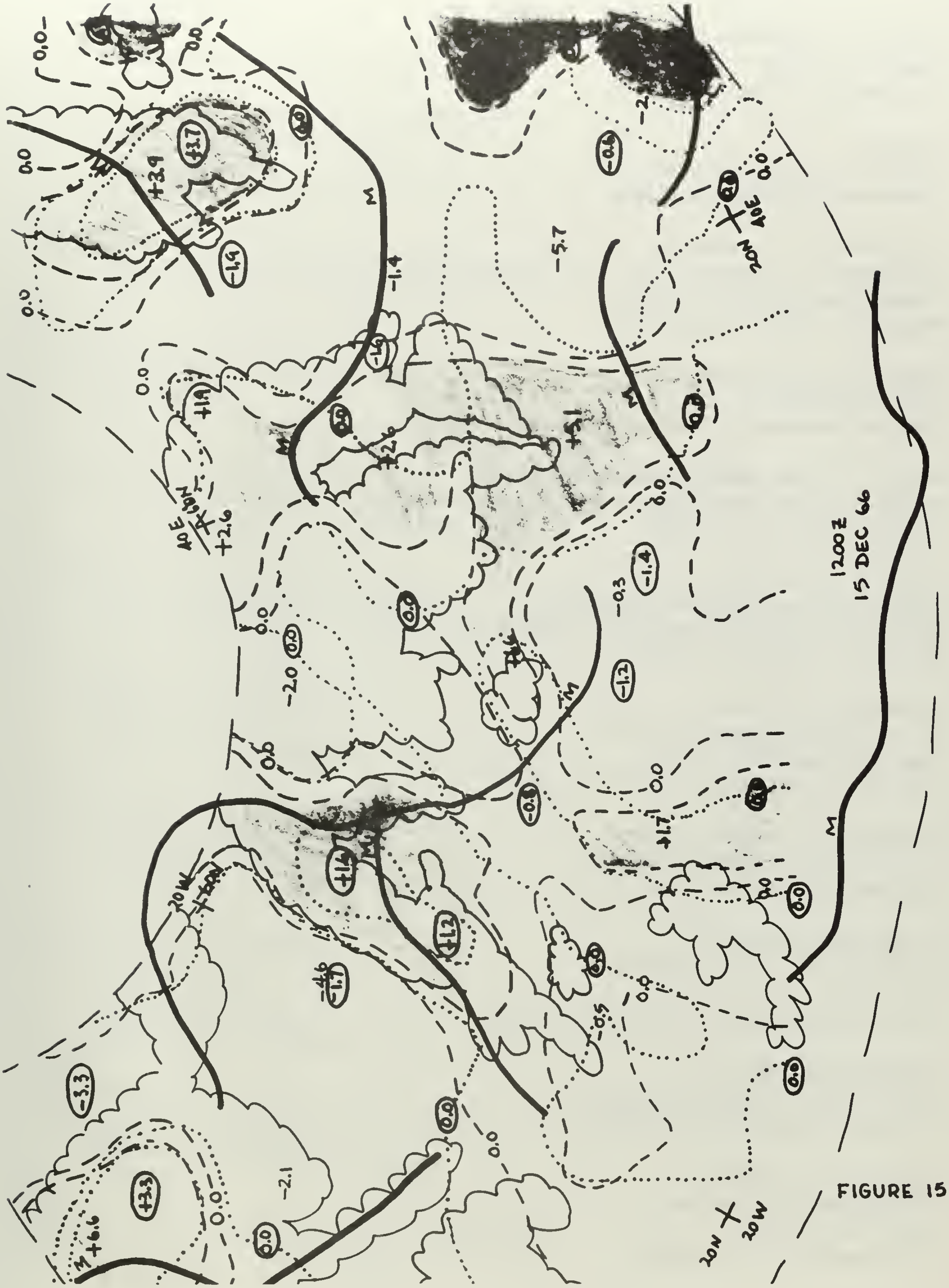

FIGURE 15E

INITIAL DISTRIBUTION LIST

		No. Copies
1.	Defense Documentation Center Cameron Station Alexandria, Virginia 22314	20
2.	Library Naval Postgraduate School Monterey, California 93940	2
3.	Professor R. J. Renard Department of Meteorology and Oceanography Naval Postgraduate School Monterey, California 93940	10
4.	LCDR J. W. Shoemyer COMASWGRU Three FPO San Francisco California 96601	5
5.	Office of the Naval Weather Service Naval Station (Washington Navy Yard Annex) Washington, D. C. 20390	1
6.	Officer in Charge Naval Weather Research Facility Naval Air Station, Building R-48 Norfolk, Virginia 23511	1
7.	Commanding Officer U. S. Fleet Weather Central Box 12, COMNAVMARIANAS FPO San Francisco, California 96601	1
8.	Commanding Officer U. S. Fleet Weather Central FPO Seattle, Washington 98790	1
9.	Commanding Officer U. S. Fleet Weather Central Box 10 FPO San Francisco, California 96610	1
10.	Commanding Officer U. S. Fleet Weather Central FPO New York, New York 09540	1
11.	Commanding Officer Fleet Weather Central Navy Department Washington, D. C. 20390	1

		No. Copies
12.	Commanding Officer Fleet Weather Central Naval Air Station Alameda, California 94501	1
13.	Commanding Officer and Director Navy Electronics Laboratory Attn: Code 2230 San Diego, California 92152	1
14.	Officer in Charge U. S. Fleet Weather Facility FPO New York, New York 09597	1
15.	Officer in Charge U. S. Fleet Weather Facility Box 72 FPO New York, New York 09510	1
16.	Officer in Charge U. S. Fleet Weather Facility FPO San Francisco, California 96662	1
17.	Officer in Charge U. S. Fleet Weather Facility FPO San Francisco, California 96652	1
18.	Officer in Charge Fleet Weather Facility Naval Air Station San Diego, California 92135	1
19.	Officer in Charge Fleet Weather Facility Naval Air Station Quonset Point, Rhode Island 02819	1
20.	Officer in Charge Fleet Weather Facility P.O. Box 85 Naval Air Station Jacksonville, Florida 32212	1
21.	Officer in Charge Fleet Numerical Weather Facility Naval Postgraduate School Monterey, California 93940	1
22.	Director, Naval Research Laboratory Attn: Tech. Services Info. Officer Washington, D. C. 20390	1

No. Copies

23. Office of Naval Research
Department of the Navy
Washington, D. C. 20360 — 1

DOCUMENT CONTROL DATA - R&D

(Security classification of title, body of abstract and indexing annotation must be entered when the overall report is classified)

1. ORIGINATING ACTIVITY *(Corporate author)*
Naval Postgraduate School
Monterey, California

2a. REPORT SECURITY CLASSIFICATION
UNCLASSIFIED

2b. GROUP

3. REPORT TITLE
INTERRELATIONSHIPS BETWEEN SATELLITE-OBSERVED CLOUD PATTERNS, NUMERICALLY ANALYZED BAROCLINICITY AND VERTICAL MOTION

4. DESCRIPTIVE NOTES *(Type of report and inclusive dates)*
Thesis

5. AUTHOR(S) *(Last name, first name, initial)*
SHOEMYER, James W.

6. REPORT DATE	7a. TOTAL NO. OF PAGES	7b. NO. OF REFS
June 1967	82	16

8a. CONTRACT OR GRANT NO.	9a. ORIGINATOR'S REPORT NUMBER(S)
b. PROJECT NO.	
c.	9b. OTHER REPORT NO(S) *(Any other numbers that may be assigned this report)*
d.	

10. AVAILABILITY/LIMITATION NOTICES
This document is subject to special export controls and each transmittal to foreign government or foreign nationals may be made only with prior approval of the U. S. Naval Postgraduate School.

11. SUPPLEMENTARY NOTES	12. SPONSORING MILITARY ACTIVITY
	Naval Postgraduate School

13. ABSTRACT

Numerically analyzed baroclinicity, an operational product of Fleet Numerical Weather Facility (FNWF), Monterey, California, is related to cloud patterns depicted on ESSA III nephanalyses for the Atlantic-European and Pacific-North American areas during the period 7-17 December 1966. In addition, interrelations between the numerically analyzed fronts, satellite cloud observations and FNWF 850-mb and 500-mb vertical motion fields are presented. Hyperbaroclinic zones are found to contain a greater percentage of clouds than areas outside these zones at all latitudes from 15-60 N. For instance, 61% (44%) of the average hyperbaroclinic zone in the Pacific-North American (Atlantic-European) area is covered by more than .5 clouds while only 30% (28%) of the adjacent quasi barotropic zones show similar cloudiness. The FNWF fronts and cloud bands are found most closely related, in orientation and intensity, in the dense-data Atlantic Ocean area. More clouds are found to occur in regions of ascent than in regions of descent, the ratio being 2 over land and 1.5 over ocean areas, but the correlation of vertical motion and percentage of cloud cover is not simple or necessarily positive.

DD FORM 1 JAN 64 1473

14 KEY WORDS	LINK A		LINK B		LINK C	
	ROLE	WT	ROLE	WT	ROLE	WT
Satellite Meteorology						
Vertical Motion						
Baroclinicity						
Clouds						
Fronts